CHARACTERIZATION AND REDUCTION OF FRICTION IN A HYBRID TRANSMISSION:

SURFACE ENGINEERING FOR ENVIRONMENTAL AND PERFORMANCE BENEFIT

BY

MARK DUBOIS

B.ENG. (MECH. ENG.)

A Thesis Submitted to the School of Graduate Studies in Partial Fulfilment of the Requirements for the Degree Master of Applied Science.

MASTER OF APPLIED SCIENCE (2012) McMASTER UNIVERSITY

(MECHANICAL ENGINEERING) HAMILTON, ONTARIO, CANADA

TITLE: CHARACTERIZATION AND REDUCTION OF FRICTION IN A HYBRID TRANSMISSION

AUTHOR: MARK DUBOIS

B.ENG (MECH. ENG.) McMASTER UNIVERSITY

SUPERVISOR: DR. STEPHEN VELDHUIS

NUMBER OF PAGES: VIII, 80

Abstract

The aim of this study was to explore environmentally friendly solutions to reduce the friction present in automotive transmissions.

A 2005 Ford Escape Hybrid transmission was used in this study to establish reasonable operating conditions for the gear surfaces.

Background on gear operation and surface interaction was studied to understand the nature of the contact between the gear surfaces. Based on this, a mathematical model of gear interaction was developed and used to bracket the loading conditions of the gear tooth interface to be up to 1.5GPa of contact pressure with 2m/s relative sliding velocity. This information was used to aid in the identification of suitable surface engineering technologies and set the operating conditions for reciprocating tribometer based measurements.

Additionally, tribological tests were performed on pin-on-disc samples which were treated with various surface treatments. The resulting wear surfaces were then studied using optical and Scanning Electron Microscopy (SEM) as well as Raman Spectroscopy. These techniques were used to better understand the mechanisms associated with wear and the role that the surface treatments played in reducing wear. Based on the testing performed, the best surface treatment for this application was a super finishing process. This process also met cost and environmental constraints. An in-house dynamometer was also developed to be used in the future full scale testing of a transmission.

To my parents, Dr.'s David and Denise DuBois:

To whom all things I owe.

Acknowledgements

This research would not have been possible without the guidance of my supervisor Dr. Stephen Veldhuis and the use of his facilities in the MMRI and CMHT at McMaster University. I would also like to thank Dr. German Fox-Rabinovich and Dr. Manuel Abad for their technical input and assistance in my work.

Furthermore, all of the fabrication which was made throughout this research owes its gratitude to the help of Terry Wagg, Mark MacKenzie, Ron Lodewyks, Jim McLaren and JP Talon.

Special mention must be given to my fellow colleagues and friends Simon Oomen-Hurst, Yu Song, Youssef Ziada, Dr. Stephen Andrew Gadsden, Jeff Sylvester and Cam Fisher – for their time and help to overcome many obstacles.

This research study would like to acknowledge the corporate support of Brycoat Inc., Oerlikon Balzers, and Metal Improvement Company for their services in coating the samples. Testing was performed at the University of Windsor with the support of Dr. A. Alpas in his Tribology Research Center.

Lastly, I would like to thank my thesis committee, Dr. Habibi and Dr. Sklad for taking the time to review my work. As iron sharpens iron, so too does the growth and success of an engineer depend on the support of fellow engineers

Table of Contents

Table of Figures

List of Tables:

Introduction

In our automotive dependant world, where fossil-fuel resources are depleting, cost and fuel economy are significant concerns to consumers when buying a car. Friction is a major concern to vehicle efficiency because it absorbs nearly 10% of the input energy [1]. Consequently, it is the goal of this study to reduce these losses observed in the parallel-series hybrid transmission, found in the 2005 Ford Escape Hybrid vehicle. This specific transmission was selected because it is topically interesting and is one of the automotive industries' developing technologies within the growing market segment of hybrid vehicles. While the theory applied in this study has relevance to gear tooth sliding in nearly every commercial vehicle, this work is focussed on the operating characteristics of a hybrid vehicle. The challenge is to find a cost effective, environmentally friendly solution to reducing the friction observed in the aforementioned transmission. Several approaches to reducing friction exist. This study focuses on the surface treatment of gears to enhance their performance. Surface engineering includes polishing, texturing, hardening as well as coating. These technologies will be explored because they incur minimal changes to the design of the system. They do not change the shape, material, forces or any other design conditions within the engine, constraints which have not been altered for this project. If successful, the results from this study will benefit the manufacturer, consumer and environment alike; by bringing forward a new method to select coatings and fabricate automotive gears that will reduce production costs, increase fuel economy, improve component longevity and reliability, and reduce the footprint these vehicles have on the environment.

The success of this study is measured by its ability to address these three key factors:

ONE – Understanding Friction

The characterization of friction in the transmission through full system modeling is important to understand the behaviour of the transmission. By developing a mathematical model for the system, and obtaining a transfer function from empirical tests, it is possible to differentiate the components which contribute to its losses; such as: inertial forces, bearing losses, fluid turbulence and friction observed at the gear flank face. In doing this, the contribution sliding friction makes to the system's performance on a wide scale can be seen.

TWO – Technologies to Reduce Sliding Friction

This study focuses on the application of surface coatings to the gear flank faces. It is understood that applying a coating may have a positive effect on the performance of the transmission. It is suggested that in doing so, the friction losses would be reduced, which in turn would improve vehicle performance as well as increase fuel economy. With less friction present, the sliding interface may incur less wear which then suggests that component longevity may be increased. These, as well as many other positive attributes suggest that there may be a cascading effect of positive results and cost savings from the application of coatings. Coating selection is based on performance characteristics as well as its environmental impact and cost. A tribometer, available at the University of Windsor, will be used for testing to compare the friction performance and wear resistance of each of the selected coatings.

THREE – Improve Environmental Impact.

Notwithstanding the potential performance benefits from some coatings, all of the efforts of this research and of the Green Auto Power Train research group are to achieve this in a manner which advances hybrid technology and maintains, if not lessens, its overall environmental impact. As such, an additional goal is to achieve competitive performance increases through the use of environmentally friendly coatings or technologies.

Using mathematical models of the transmission, the environmental conditions of meshing gear teeth are calculated. From this data, technical requirements for coating selection are established and a group of surface treatments are selected. Using a tribometer, these coatings will then be tested in a controlled environment and compared based on their frictional and wear performance.

An in-house dynamometer is available for use to numerically model the losses in a transmission. With the unaltered transmission fully modelled, the best selected surface treatment may then be applied to the transmission. The motive of this is to successfully transfer the performance improvement observed in the tribology experiments to a full-scale transmission. As an illustration, if a 20% reduction in friction can be realized through a particular surface treatment and flank face friction contributes to 20% of the overall frictional losses, then a 4% improvement would be expected in full scale transmission tests. If so, the test will demonstrate that the coating application has a direct positive result on the performance of the transmission.

Background Research

An overview of the related research which has recently taken place which has contributed to the formation of this project is summarized here as background. The works collected here cover the key subjects of this research and provide a basis upon which results can be analyzed and reasoned. It is important to learn about gear tooth stress analysis, friction modeling, conventional tribological testing procedures, and what coating applications have been tested.

1.1. (Contact) Stress Analysis /FEM /FEA

A number of researchers have contributed their own efforts and findings to better understand the dynamics and stresses that gear teeth undergo. Many apply models in computer software in order to analyze various dynamics of the gears in mesh. David Sell used this approach in order to investigate contact stresses in four mesh positions [2]. His work considered the tooth deflection in the calculations and maps the loaded zones and how the stress is distributed throughout the tooth. This is important so as to understand what loads are reasonable, and how gears respond.

A similar study was reported by Ali Raad Hassan in his research on spur gear teeth in mesh. Instead of only four mesh positions, Hassan considers ten positions in 3˚ increments [3]. This takes the analysis to a more accurate level where the flow of the stresses is clearer. It is likely that 3˚ increments were chosen for the sake of time or computing power, and that points in between may be interpolated. Using Finite Element Analysis (FEA), the tooth root stresses, Von-Mises stresses and localized contact stresses were calculated. This was valuable insight and set the design parameters for the surface of the gear.

His work demonstrates how to calculate the area of contact for a spur gear tooth.

$$a = 2\sqrt{\frac{W(1-v_1^2)/E_1 + (1-v_2^2)/E_2}{F\pi(1/R_1 + 1/R_2)}} \qquad \text{Equation 1.1.1}$$

where a is the contact circle radius, W is the load, v, $E \, and \, R$ are the respective poisson's ratio, Modulus of Elasticity, radius of curvature for the interfacing surfaces and F is the face width of the gear as well as calculate the maximum contact stress observed at the center of the contact region:

$$\sigma_o = \sqrt{\frac{W(1/R_1 + 1/R_2)}{F\pi[(1 - v_1^2)/E_1 + (1 - v_2^2)/E_2]}} \qquad \text{Equation 1.1.2}$$

This is important for the appropriate calculation of contact pressures observed during different loading conditions. Based on this analysis contact stresses have been noted to reach values as high as 1.5GPa [3].

1.2. Friction Modeling

With load values defined, models made and the stress distributions mapped for loaded gears, it is useful to then begin to study the behaviour of friction. This has been studied and modelled based on theory, tribological tests as well as tests on a dynamometer. Each approach is valuable and relevant to the different stages of this project.

Friction losses for a gear drive can be estimated using two analytical methods and empirical analysis. Clapp [4] approached the calculation by evaluating the difference between the torque in and the torque out of two torque shafts connected by a gear set. Merrit [5] studied the specific frictional resistance observed by the gear teeth in contact with each other. Professor A.C. Rao investigated both approaches for accuracy. Rao concluded that Clapp's approach was more conservative and that the empirical method did not follow the trends from the previous two theories [6]. However, in the empirical tests, he also discussed how each of the component losses may be isolated through specific tests. This was described by a combination of fluid churning, sliding friction and bearing losses. He further discussed that by measuring the power input and power output, the internal mechanics can be modeled. Running multi-speed tests, no-load and unloaded helped determine the bearing losses and the losses in the motor. Subtracting these two from the output data gave a value for the losses due to the gears. From this, a coefficient of friction (CoF) may be calculated. Also, by changing the lubricant can change the viscosity in the transmission, the fluidic losses can also be modelled.

A. Mihalidis and his research students were able to further understand the friction observed between gears [7] empirically. This research started off with the same approach as Hassan's to calculate contact stresses, to calculate the theoretical stresses observed, but then goes further to model and measure friction coefficients on a FZG test rig. The tests were performed at speeds between 1500 and 3500RPM and loads ranging from 100 to 500Nm. The results indicate how the Hertzian contact zone is incorporated into the determination of the CoF. By knowing the transmitted speeds and loads, and isolating the gear friction from bearing losses or turbulent losses the CoF could be calculated. This work was successful in modeling the gear tooth sliding friction, and estimates the CoF to be near 0.06 – 0.03. This of course will vary based on setup and on the surface of the gears, but gives a good perspective for realistic coefficients.

1.3. Surface Engineering

Surface engineering encompasses a wide range of technologies used to improve the performance of a surface for a given application. The technologies explored in it have considerable value to the potential reduction of friction found in transmissions. Hardening, texturing and coating surfaces all have the potential to improve the frictional performance by reducing the CoF.

As discussed above, the CoF may be calculated and modeled through transmission testing. The results found are valuable, but may be altered or improved based on the treatment and coating application of the gear surfaces. R. Martins presented an excellent example of using coatings to improve the scuffing load capacity and performance of gears using an FZG test. Martins work applies MoS_2/Ti and C/Cr to FZG gears and tests them for 4 hours, running at 1500 and 3000RPM and monitors the wear and friction in lubricated conditions. His work does not report the specific roughness of the gears, but comments that a CoF of 0.04 was achieved with the MoS_2/Ti coating. Tests show a 19% increase in transmitted power from the C/Cr coating compared to the uncoated, and a 40% increase from the MoS_2/Ti coating [8,9,10,11].

Other coatings have been tested for tribological improvement [12,13,14] as well as other methods of friction reduction. Podgornik explored how coatings perform while in contact with different treated surfaces. He performed pin-on disc experiments to understand how WC/C may be affected by different lubricating regimes. The findings from this work showed that coating-on-coating contacts experience considerable wear and friction [15]. The best interface was shown to be coating-on-steel. Podgornik concludes that part of this is because the coating-on-coating interface does not allow for a 3rd body tribofilm to be produced. This tribofilm is the key to the reduction of friction and the smooth sliding between the interfaces [16].

Li Xiao completed his Ph.D. thesis at the Chalmers University of Technology investigating the key parameters to good tribological performance in gear applications [17]. His experiments were conducted on a gear shaver machine which is designed to have two double crowned rollers rotate in contact with each other in the same direction, at different speeds. This was his approximation to the gear tooth interaction.

It was with this apparatus that he investigated the friction and wear performance of surface topography. His sample's surface treatment ranged from grinding, shotpeening, phosphating, chemical deburring and Diamond-Like Carbon (DLC) coating. His results further support the use of super-polishing as a method of reducing friction. However, research indicates an optimum point when a high-polished surface with extremely low roughness begins to perform poorer than the others [18]. This is explained through the role that surface roughness plays in fluid retention between the contacts. Surface finish also impacts dry sliding but the mechanisms involved are different.

1.4. Lubricants

Lastly, exploring lubricating fluid technology can also have a significant effect on the performance of the transmission. By altering the viscosity, viscosity index, additives, and other properties, it is possible to change the function and performance of the lubricating fluid. Researchers like Kozma [19] have investigated the tribological performance of environmentally friendly lubricants such as mineral oil, vegetable oil and rapeseed oil as lubricating fluids for gear applications. The performance of these oils was analyzed for its ability to reduce scuffing on the sliding surfaces. This encourages the development of alternative base oils in automotive applications and would be a valuable way to have considerable impact on the use of non-renewable resources.

Other researchers like Kalin [20] and companies like Terresolve [21] are also exploring the use of environmentally friendly oils as base stock for lubricating fluids in various applications. This technology has the potential to greatly improve the environmental implications, recyclability, and reduce the toxicity of industrial fluids. It is not within the scope of this study to experiment with these technologies. But their development is exciting to see for the progress of greener vehicles.

This background research presents the conventional approaches to studying friction between gear teeth. It discusses how meshing gear teeth have previously been modelled, and the behaviours which may be expected from them. It also outlines the key variables to focus on and some of the testing conditions previously observed. Various coatings have been tested with moderate success, and that the use of liquid lubricants is another avenue to explore for minimizing gear-box friction and environmental impact.

Chapter 2. Friction and Wear Theory

2.1. Dry Sliding Theory

Friction between sliding surfaces depends heavily on the materials involved. At a microscopic scale, all surfaces have a measurable roughness which interferes with the opposing surface. Empirical studies of simple sliding friction shows a direct correlation between friction force and normal force. This holds true within reasonable bounds. Shaw [22] explains that this friction force value is in actuality a summation of all the interfering asperities (of the softer material) shearing under stress. And, as roughness decreases, fewer and fewer asperities are sheared at a given time, but are under proportionately higher loads. Therefore, the total frictional force, F_f, is derived from the real area, A_{real}, multiplied by the shear strength of the softer local material τ_{soft}.

$$A_{real} = \sum_{i}^{n} A_i \qquad \text{Equation 2.1.1}$$

$$F_f = \tau_{soft} * A_{real} \qquad \text{Equation 2.1.2}$$

where A_{real} is the summation of all asperities in contact.

It is because of this deduction that simple sliding friction is shown to be independent of the apparent surface area. This linear relationship holds true within reasonable bounds, but is non-linear upon its extremities; which exist under substantially low / high surface roughness, hardness, sliding velocity, and temperature. This too can be true for contact pressure, when the contact stress exceeds the softer material shear stress. Shaw outlines this phenomenon and discusses the three distinct behaviours using the information shown in Figure 2.1.

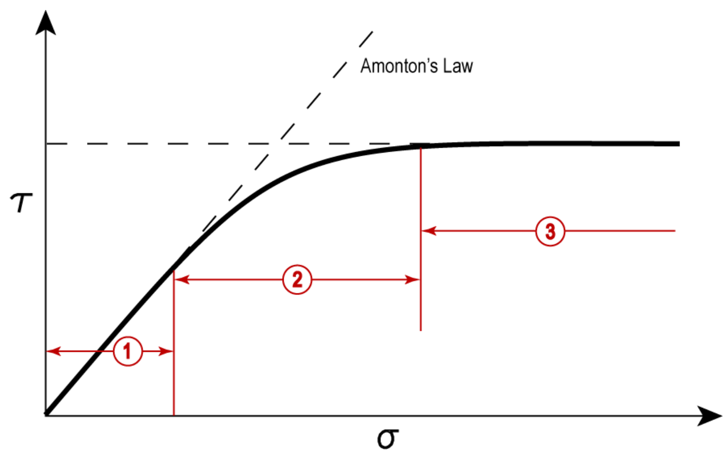

Figure 2.1 Dry Sliding Regions (adapted from [2])

1. $A_{real} \ll A_{observed}$, Plastic flow, asperity only, $\mu = \frac{\tau}{\sigma} = const.$
2. $A_{real} < A_{observed}$, Plastic flow in bulk material, metal cutting,
   $\mu = \frac{\tau}{\sigma}$, this decreases with increasing load.
3. $A_{real} = A_{observed}$, τ is independent of σ.

For gear applications, the loads will not exceed the first region. Other factors such as velocity, temperature, and contact pressure can affect the friction observed, but only in extreme cases. Within the linear region, μ is the ratio between shear strength and yield strength. In *Friction and Wear of Material*, Rabinowicz derives [23]:

$$\mu \cong \frac{\tau}{\sigma}, \because \sigma \propto H, \quad \therefore \mu \cong \frac{\tau}{H}$$

Where μ is the CoF, τ is the shear strength of the material, σ is the yield strength of the material and H is the hardness of the material.

The CoF, μ, naturally ranges between 0.17 and 0.5 for steel on steel contact. From this theory we can also appreciate the significance of surface hardness and shear strength on the variation in friction coefficients. Thus, in order to minimize the CoF, the hardness, H, must increase, and/or decrease the shear strength, τ, of the material. Since this does not occur naturally, there is a need to develop a composite of materials to achieve friction reduction. This illustrates very effectively how coatings may be useful for various applications. With the application of lubricious coatings, the surface shear strength is reduced, while maintaining high yield strength from the substrate. This also illustrates how coating failure may be detected. The friction and wear behaviour of the coated surface may be predicted according to Figure 2.2:

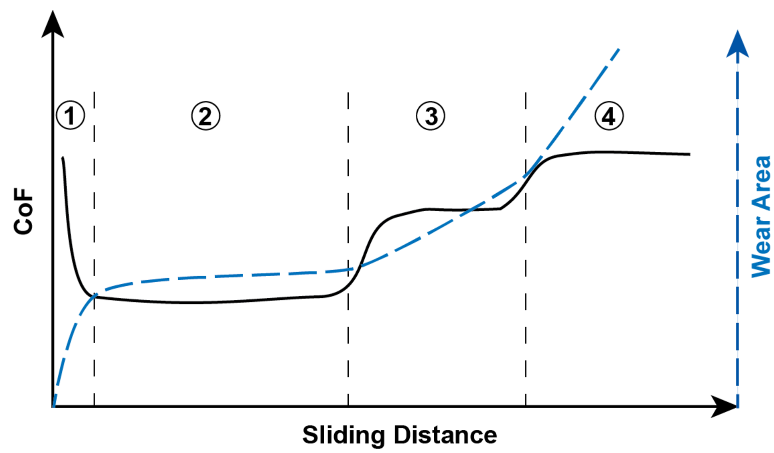

Figure 2.2 Friction and Wear Rate Changes Due to Coating Failure

In Region 1, there is a rapid decrease in friction and a rapid increase in wear area. This is referred to as the *break-in* period, where the interfacing asperities are broken, as described above. Ideally, region 2 is the longest and steadiest period of performance for a component. This is referred to as the steady-wear region [24], where the sliding surfaces are operating within their designed conditions. These are the design conditions of the component. Region 3 and 4 indicate an increase in friction and wear rate due to the failure of one or both of the coatings. This is due to the change in contact physics. Instead of a coated surface sliding against another coated surface, one of the coatings has worn through so that there is now a coating-on-substrate or substrate-on-substrate environment. Each of these has a unique friction coefficient. Region 4 exists when both surfaces have been applied to a coating. This is recognized as component failure because the CoF and wear rate rapidly increases until catastrophic failure.

Rabinowicz [23] discusses in his book how friction and wear are proportional to each other. With this relationship, both friction and wear will be used as a means of comparing coating performance during testing.

2.1.1. Static and Kinetic Friction

Static friction relates to the force required to overcome stiction and make a stationary object move. Kinetic friction relates to the resistive force required to allow a moving object to continue to move at a steady speed. The established method to determine these coefficients is to use an angled plane as shown in Figure 2.3.

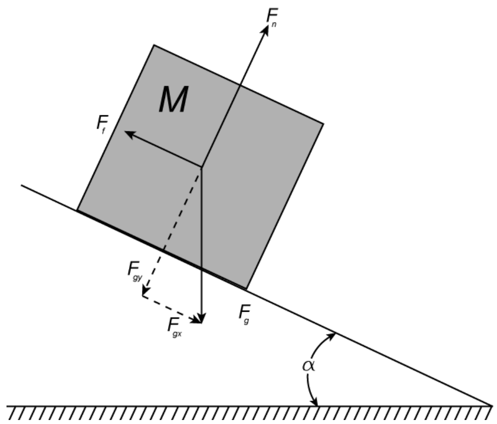

Figure 2.3 Mass on Angled Plane

The angle which causes a stationary object to begin motion is used to calculate the static CoF.

For kinetic friction, an object is given a small push to overcome the static resistance and is measured to observe which angle allows for a constant velocity. A constant velocity establishes that the gravitational force and the frictional force are equivalent and in balance, thus, no acceleration is present in the system.

Ordinarily, kinetic friction is significantly less than static friction. So when the sliding velocity of two objects is low, or the applied force is in between the critical values of the two friction forces, there exists a switching behaviour referred to as stick-slip. A mechanism, shown in Figure 2.4, may be used to illustrate this behaviour. Booser models the 1-D motion of a mass on a plane which is being pulled by a prime mover at a steady speed. The mover and the mass are connected by a spring damper [25].

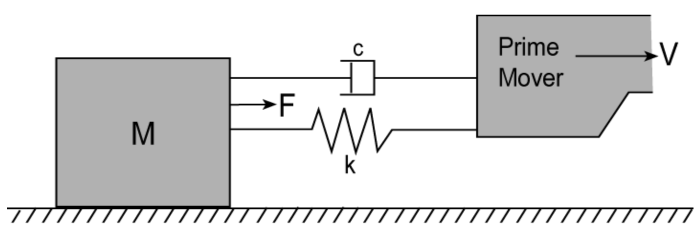

Figure 2.4 Prime Mover Schematic [adapted from 25]

Booser explains how this setup creates a build-up and release of tension because of the jumping between μ_k and μ_s. The frequency and magnitude of this bouncing depends on the sliding speed, weight of the object, spring stiffness, k, damping effects, c, and the difference between μ_k and μ_s. Stick-slip will always exist, but can be minimized or controlled to tolerable limits by changing the values of these variables.

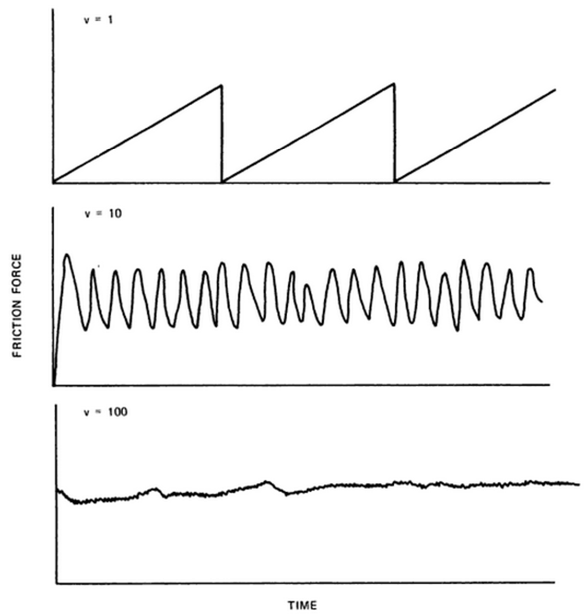

Figure 2.5 Friction Forces Measured of Object Experiencing Stick-slip at Various Speeds [taken from 4]

Figure 2.5 illustrates the friction force observed by the sliding mass as the prime mover pulls the system along at increasing velocities. This shows that there exists a critical resistive force which must be overcome to allow the object to move. During low velocity regions, the difference between static friction and kinetic friction creates this highly discontinuous movement because the elastic system switches between a sliding and stationary state. Yet when the sliding velocity increases, the motion is predominantly influenced by kinetic friction and creates a relatively consistent friction force. This illustrates the real motion of sliding of elastic objects, and will be valuable to understand for later sections.

2.2. Wet Sliding Theory

When a fluid is introduced between two sliding surfaces, the fluid alleviates some of the asperity contacts which reduces the friction force observed. The faster they slide, the thicker the fluid film becomes between them. This, in turn, further reduces the friction. This has been illustrated through the Stribeck curve as shown in Figure 2.6.

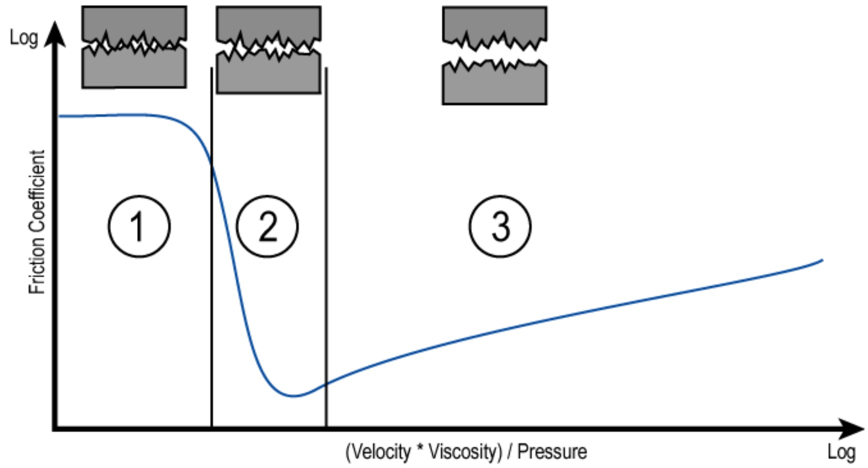

Figure 2.6 Stribeck Curve (adapted from [25])

The ratio between the fluid film thickness and the surface roughness, noted by λ, defines the sliding regime of the surfaces.

$$\lambda = \frac{h_0}{\sqrt{\sigma_A^2 + \sigma_B^2}} \qquad \text{Equation 2.2.1}$$

where h_0 is the minimum fluid film thickness and σ_A and σ_B are the RMS roughness of the respective surfaces. In region 1, when λ is below unity, significant asperity contact interferes with the sliding. Above 3, sliding is completely free of surface contact and is pure fluid friction [20]. In this region, friction no longer depends on the sliding material. Instead, friction is dictated by the velocity, viscosity and pressure. Viscosity varies depending on the fluid properties and change uniquely as temperature changes. Between these regions exists a mixed boundary lubrication, where there is both a fluid boundary layer as well as some asperity contact. Logically, the higher λ is, the lower the wear and friction forces will be.

1. Boundary Lubrication ($\lambda < 1$)
2. Mixed Lubrication ($\lambda \sim 1$)
3. Hydrodynamic Lubrication ($\lambda > 3$)

The parameter λ is the term which separates the primary sliding regimes. This study remains within regions 1 and 2 of the Stribeck curve.

The Stribeck curve shows what affect the lubricant boundary layer has on the CoF. This rapid reduction in the CoF is achieved because it minimizes the contact of the surface asperities under sliding, and stimulates flow which is dominated by the shear strength of the lubricant. As the surface separation increases, the CoF is dictated predominantly by the separating fluid. This, in turn, means that the mechanical properties of the surfaces become insignificant. Regime 3 illustrates a slight and gradual increase in CoF because of the fluidic properties changing due to viscosity changes (commonly due to temperature) and excessive velocity. This final stage is particular to each fluid, but the trend is common. Regime 3 is not of focus for this study as the sliding velocities in this study are not great enough to reach this region.

The design of a lubricant is a complex science of mixing many additives, in the right amounts, to get the desired performance characteristics. The lubricant clearly has a significant impact on the performance of the tests but is not explored in depth because the focus was to explore effective surface engineering technologies.

2.3. Wear

Wear is a phenomenon which is still only understood at an empirical level. It is commonly distinguished by its different mechanisms, which include mechanical, chemical and thermal wear. This study focusses on the behaviour of mechanical wear because it is the dominant mechanism for material and surface failure of sliding surfaces. Mechanical wear can be separated into abrasive, fatigue and adhesive wear.

2.3.1. Abrasive Wear

Through testing, abrasive wear is shown to be predominantly dependant on counterpart material, contact pressure, sliding velocity, contact shape and environment (temperature, humidity, wet/dry sliding). Abrasion is one of the most aggressive forms of wear and is the result of a mechanical breakdown at the interface between the asperities in contact. This follows the theories described in Section 2.1, under the condition that one of the surfaces is much harder than the other. In general, the wear of a material is:

$$W = \frac{KLD}{H} \qquad \text{Equation 2.3.1}$$

where W is the wear volume, K is the wear coefficient, L is the contact load, D is the sliding distance and H is the indentation hardness[24]. When the surface hardness of the interacting surfaces are similar, the mechanism becomes less well-defined. This relationship is a general observation which begins to breakdown in complex scenarios and is sensitive to errors in testing, such as those introduced by variation in lubricants, and the presence of impurities or particle debris. This is mostly observed during the early stages of sliding and may be illustrated in gear applications through scratching, but can often be alleviated by adding a lubricant.

2.3.2. Fatigue Wear

Due to the repeated contact loads, cracks may grow on and below the surface of the gear. Surface fatigue wear occur over millions of cycles of repeated loads, but can have catastrophic results to the components. Things like pitting and spalling may occur due to fatigue wear and is a result of the improper design of the gears or an overloading of the components.

In discussing the theories of dry sliding friction, it is agreed that key factor which contribute to dry sliding friction is the ratio between material yield strength and surface shear strength. This clearly illustrates the opportunity that coatings have to alleviate frictional forces between surfaces in contact. Also, lubricants can also have a significant impact on friction, depending on the sliding regime. This is also driven by the load, sliding velocity, and roughness of the materials.

2.3.3. Adhesive Wear

Friction theory described in Section 2.1 describes only one of the theories to friction. The second debated theory is based on the adhesion of surfaces in contact under pressure [23,26]. This phenomena is a significant mechanism present during sliding which describes how adhesive wear operates, and how particles may be removed from the surface by the bonding to the mating surface. Common forms of adhesive wear are illustrated in gear applications through scuffing.

What can be observed from this discussion is that friction and wear are the result of surface interactions, and are largely depend on the same variables. Rabinowicz comments on the correlation between friction and wear. He describes that, within adhesive wear, the material's specific wear coefficient is proportional to its friction coefficient [23]. This emphasizes that measuring wear will give a good indication to the frictional performance of the material and vise-versa.

Chapter 3. Gears

3.1. Types of Gears

In automotive transmissions, parallel-axis gears are used to transmit the power from the engine through the drive train to the differential. These can be combined to produce a wide range of gear ratio. Historically, all of these gears were made with straight tooth faces, which as referred to as spur gears. As the functions became more complex, other designs such as helical, bevel, and hypoid gears were developed. Examples are provided in Figure 3.1.

Spur

Helical

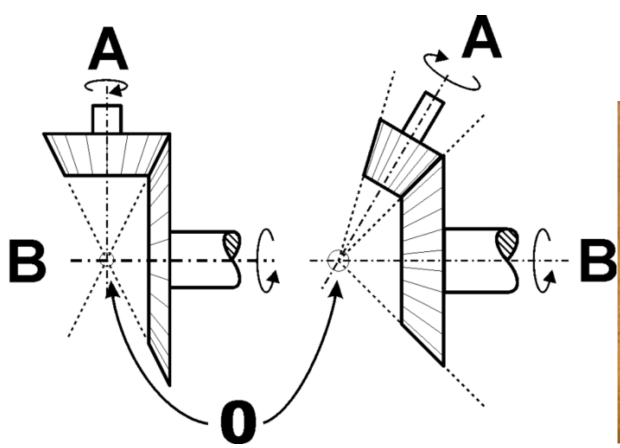

Bevel

Hypoid

Figure 3.1 Types of Gears

Spur and helical gears are classified as parallel-axis gears, whereas bevel and hypoid gears are considered angled-axis gears. Spur and bevel gears are similar in that they both have straight gear teeth.

This is a simple design which is easy to machine but has performance drawbacks. Figure 3.2 highlights the contact point and resolves the forces into their components.

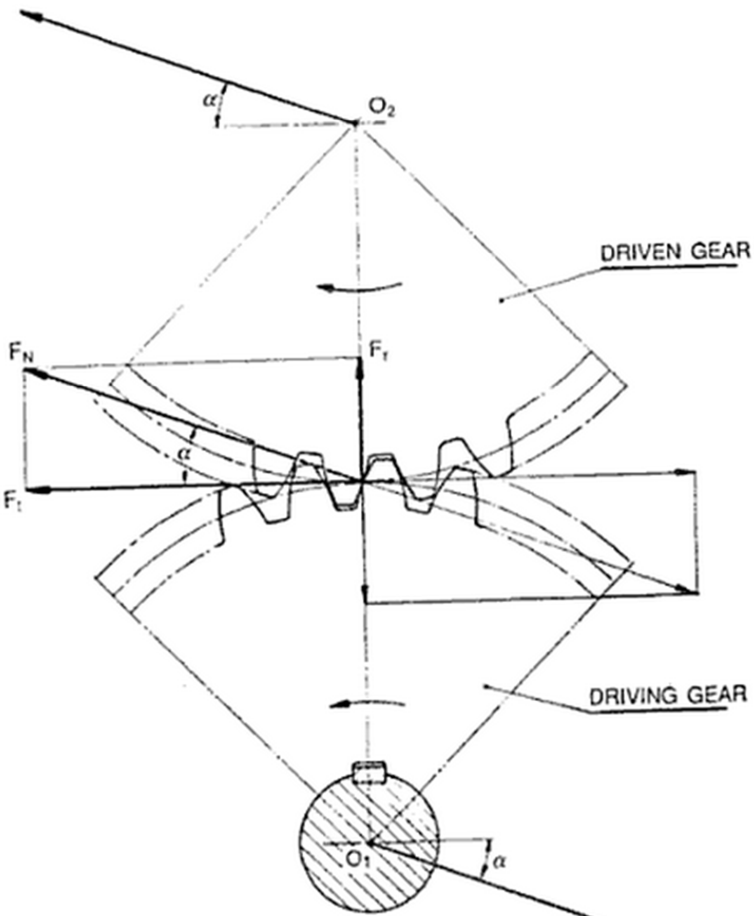

Figure 3.2 Gear Tooth Engagement [taken from 27]

The contact force observed on a spur gear can be defined by:

$$F_T = \tau_1 r_1 \qquad \text{Equation 3.1.1}$$

$$F_N = \frac{\tau_1 r_1}{\cos \rho} \qquad \text{Equation 3.1.2}$$

where F_T is the transmitted load, τ_1 is the torque, r_1 is the contact radius, F_N is the normal load and ρ is the pressure angle.

With spur gears, the teeth contact over the full width of the tooth flank face. Tooth engagement and disengagement is sudden, generating high levels of stress at the tooth base as well as at the initial contact interface. Over time, this aggressive cyclic loading may cause cracking and gear failure.

Helical gear design solves these problems by creating an angled tooth on the gear. This helix angle allows for the gear teeth to come into full engagement over a longer period of time corresponding to a longer line of contact as illustrated in Figure 3.3 with transitions occurring gradually through the entrance and exit of the gear teeth making performance smoother.

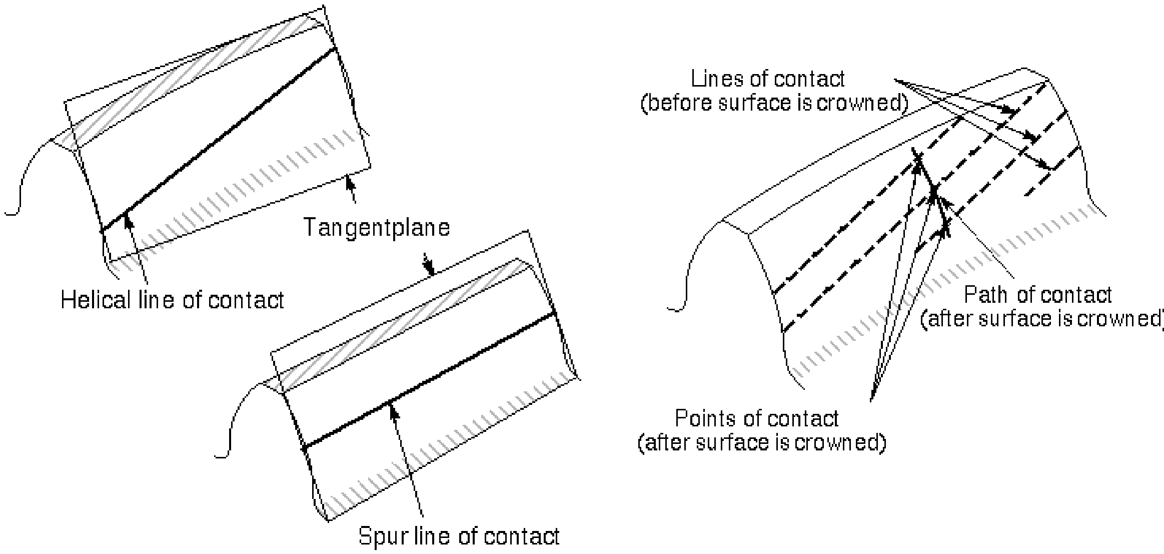

Figure 3.3 Helical Line of Contact versus Spur Gear

Helical gears also exhibit a less aggressive stress loading than observed in the spur gear and reduces the noise of the gears. However, due to the helix angle, some of the transmitted force generates an axial force on the gear. This means that some of the transmitted power is redirected into an axial load. This explains why all helical gear shafts are held using thrust bearings. One way to alleviate the load applied axially to the thrust bearing is to pair two helical gears with opposing helix angles on the same shaft. These are called herring-bone gears and help to reduce the forces observed by the bearings. The normal and axial forces generated can be calculated with the formulas provided below:

$$F_N = \frac{\tau_1 r_1}{\cos\rho}\cos\varphi \qquad \text{Equation 3.1.3}$$

$$F_A = \tau_1 r_1 \sin\varphi \qquad \text{Equation 3.1.4}$$

where φ is the helix angle and F_A is the axial force generated due to the helical tooth. All the gears taken from the Ford Hybrid transmission are helical.

3.2. Transmission (Dis) Assembly

Parallel-Series Hybrid transmissions operate very differently than manual or automatic transmissions. Both of the latter have single input, single output systems which shift power through multiple gear combinations, manually or automatically, in order to change the gear ratio; as illustrated in Figure 3.4.

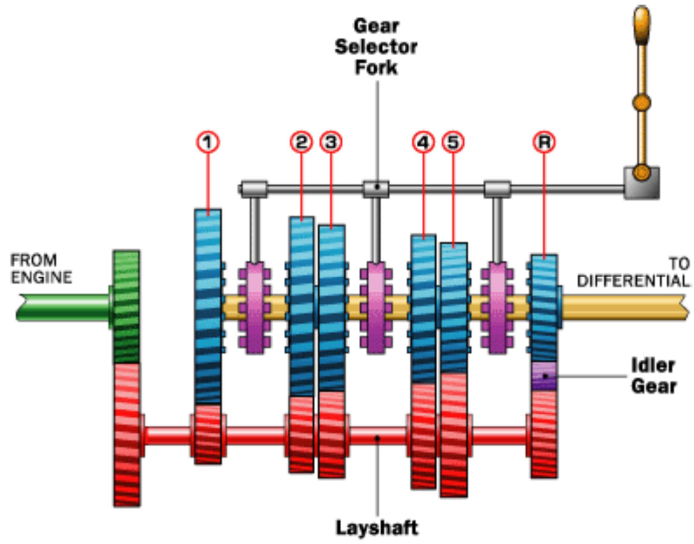

Figure 3.4 Manual Transmission [Taken from28]

The hybrid transmission used in this study functions quite differently because of the incorporation of an electric motor as a second power input. In a series-hybrid transmission, an internal combustion engine (ICE) is used to generate electrical energy. This energy is stored in batteries and powers an electric motor, which drives the wheels. While both the ICE and the motor have vital functions for the operation of the car, it is effectively an electric system. However, in this parallel hybrid transmission, both the motor and ICE operate together to drive the wheels. This is illustrated schematically in Figure 3.5.

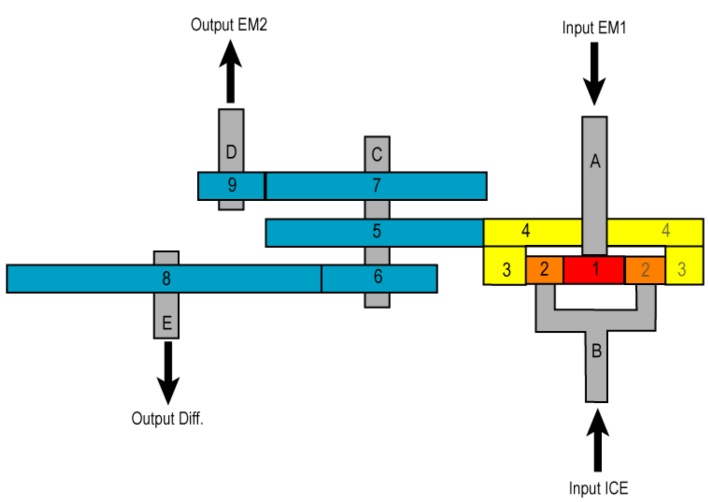

Figure 3.5 Schematic of Hybrid Gear Train

This schematic was formed through careful deconstruction of the transmission provided. Power from the motor (shaft A) and ICE (shaft B) are combined via a planetary gear set (gears 1, 2 and 3) to drive the differential (gear 8, shaft E). With this setup, there is no shifting of gears; so the driving ratio is controlled through the relative speeds of the ICE and the motor. The speed of the output may be expressed by the following equation:

$$\omega_{out} = \omega_1 \left[\frac{n_{out}}{n_1}\right]_{Input\ 2\ fixed} + \omega_2 \left[\frac{n_{out}}{n_2}\right]_{Input\ 1\ fixed} \qquad \text{Equation 3.2.1}$$

where ω is the rotational velocity and n is the number of teeth for the relative gear [29].

This setup allows for an infinite number of gear ratios, and performs multiple different functions by simply changing ratios. This setup allows the system to perform low speed, high speed and reverse driving, and acting as a generator, starter motor, and as an electric only vehicle.

This information is crucial for the modeling of the gears. Some of these measurements were obtained physically (number of teeth, weight, width, etc.) from the system shown in Figure 3.6; others were calculated based on basic relationships to other variables (gear ratio, pressure angle, pitch diameter, etc.) [27]. Other complex data, such as the moments of inertia were obtained from computer models using Autodesk Inventor. Information on the gears is summarized in Table 3.1.

Figure3.6 CAD Modeling of transmission components.

This information will be used later to calculate some of the environmental conditions the gears undergo.

Table 3.1 Transmission Information

Name	Gear	Outside Dia	Root Dia	Width	Num Teeth	Helical Angle	Pressure Angle	Hardness (HRc)	Mass (kg)	MoI (kg mm^2)
Sun	1	43.35	38.00	19.30	33	25	~21.8	56.4	0.144	38.793
Planet	2	31.36	26.01	19.30	23	25	~21.8	62.5	1.825 (engine shaft included. Gears are estimated as .086kg each)	9.838 each
Ring	3	103.00	98.90	29.50	79	25	~21.8	20.9	0.988	2684.286
Ring Output	4	95.40	81.00	21.35	38	30	~15.97	63.8	1.149 (shaft only. With Bearings(nsk6008=190g, nsk6010=261g) = 1.600kg)	1092.881
Inter from Ring Output	5	161.20	155.03	21.35	67	30	~15.97	63.0		
Inter to Diff	6	82.20	67.47	33.25	25	30	~20.03	63.0	5.864 (with 2 thrust bearings included)	17130.961
Inter to MG2	7	161.20	156.51	27.75	81	30	~16.06	62.2		
BIG Diff	8	228.80	210.00	33.25	76	30	~20.03	62.2	3.747	34963.993
Differential								63.1	6.187	12971.23
Diff Bolts								-	.605 (total. Each bolt = 38g * 16)	
MG2	9	49.53	39.90	27.75	23	30	~16.06	61.9	.715 (shaft only. With bearing(nsk-6307=.464kg) = 1.179kg)	171.995
Shaft Clamp								-	1.259	1292.465

3.3. Vehicle Performance

It is important to first establish that there are multiple loading conditions to discuss which mimic driving conditions. The transmission provided for testing was taken from a 2005 Ford Escape Hybrid. This is a mid-sized vehicle which is required to perform over a wide range of operating conditions. This vehicle has been designed to perform well during highway driving, city driving, towing, and possibly over rough terrain. The conditions which are most aggressive to the gears will be the focus of this study because these are likely the source for the onset of component failure, and because this enables testing to be conducted in a timely manner while still attaining meaningful data.

It is suggested that start up and full throttle acceleration are two noteworthy cases to examine.

Start-up can be damaging because the gears may not be properly lubricated in the first few moments and will experience dry sliding. As discussed in Section 2.1, dry sliding can have excessive surface contact which causes considerable wear and damage to the surfaces.

Full throttle acceleration is the next obvious scenario to consider because of the extremely high loads and speeds experienced. These two scenarios are not as common as steady state highway driving or city stop-and-go traffic, but these are not as aggressive to the gears as the former.

The Escape is equipped with a 155hp (@ 6000 RPM) ICE and a 94hp (@ 5000 RPM) electric motor. Paired together the vehicle has a net power output of 177 brake horsepower and 136 ft.lb (184 N·m) of torque. Under full throttle, the car can accelerate from 0 – 100km/h in 11.5s [30]. This is the most aggressive scenario the car will undergo. Highway driving may be strenuous in other forms, due to the long running time, but full throttle acceleration will be considered the focus scenario to calculate the bounds of the environmental conditions.

3.4. Materials

In order to identify the material of the gears, samples were cut and prepared for testing. Scanning Electron Microscope (SEM) test results were unable to identify the specific gear material, so more advanced testing methods were needed. Glow Discharge Optical Emission Spectroscopy (GDOES) tests and Induction-Coupled Plasma (ICP) tests are common methods, but vary in a few key manners. GDOES uses a sputtered light beam on to a ground surface to detect the elemental composition. This is a costly process, but produces confident breakdowns of the material properties. ICP dissolves material filings into a strong acid which then undergoes chemical analysis to determine the metal make up. This process is timely and requires some preliminary knowledge of the steel at hand. For this reason, GDOES test was selected, and returned reports which were entered into the CES Database. It was found to be a low-carbon, low-alloy steel with a surface hardness of 63 HRc and a substrate hardness of 29 HRc. Increased surface hardness indicates the material was either nitrided or carburized. Determining which of the two processes was used depends on the material itself. This will also have an impact on which coatings will be viable for the tests, as the hardening method will affect coating adhesion.

From the results presented in the Appendix, it was concluded that the gears were all made from the same material. Using the CES Database, it was possible to narrow the candidates down to 10 possible steels, two of which satisfy the composition constraints and other known properties[1]. Through further readings, it is found that AISI 1018, 4320, and 8620 are all common gear steels [31]. 8620 is the only one of these materials which overlaps with the identified candidates, thus, was selected as the substrate material to fabricate the test samples.

A summary is provided in Table 3.2

Table 3.2 Known properties of Gear steel identified as AISI 8620:

Surface Hardness	63 HRc 1.52e9 Pa (Vickers)
Substrate Hardness	30 HRc
Density	7.9e3 kg/m^3
Young's Modulous	205 GPa
Poisson's Ratio	.29
Composition	Fe/.18-.23C/.4-.6Cr/.4-.7Ni/.7-.9Mn/.15-.3Si/..15-.25Mo.<.035P/<.04

Now that the gear materials have been identified as AISI 8620 steel, the hardening method can now also be identified. Based on SEM test results and discussions with Dr. Fox-Rabinovich, it is likely that the gears were carburized, not nitrided. If the material had been nitrided, this would have been clearly

[1] Since all of these materials met the known parameters, and were all very similar to each other (8630, 8640, 8650, 8660, 8735, 8740), choosing one over another is likely to have little or no effect to the results

pointed out by SEM tests. Since no data supports the use of nitriding, this indicates that these gears were carburized. This information will be valuable during coating selection, presented later in Chapter 5.

3.5. Sliding velocity

In standard gear trains, the pitch line velocity is the shared velocity of two intersecting gears. It is calculated as $v = \omega r_p$, where ω is the angular velocity (rad/s) and r_p is the pitch radius (m). This is the commonly understood velocity which is used in calculations for gear trains and is highlighted in Figure 3.7. However, interacting flank faces roll and slide between each other, so a more accurate velocity must be calculated. The sliding velocity intended for testing conditions is the relative velocity observed between the flank faces of two curve surfaces.

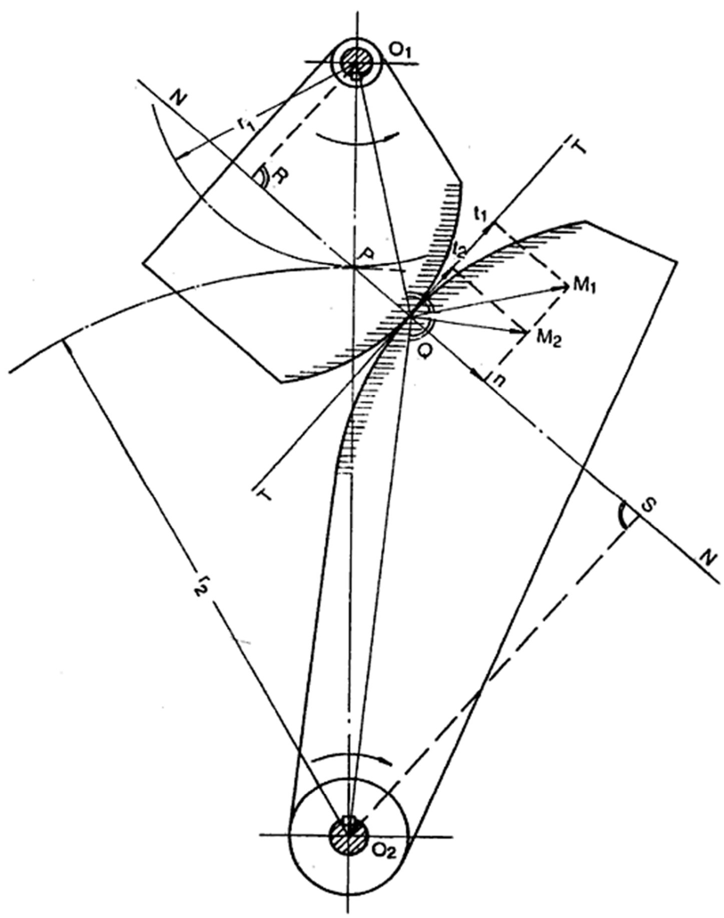

Figure 3.7 Gear Mesh Diagram to Calculate Sliding Velocity [Taken from 27]

Gitin Maitra derives this sliding contact and proves that the relative sliding velocity is written as:

$$Q_{t1} - Q_{t2} = PQ(\omega_1 + \omega_2) \qquad \text{Equation 3.5.1}$$

where ω_1 and ω_2 are the angular velocities of their respective gears, Q_{t1} and Q_{t2} are the tangential velocity vectors at the point of contact, and PQ is the linear distance the point of contact is from the pitch point [27]. Figure 3.7 [27] illustrates these terms.

Since ω_1 and ω_2 are constant for their respective gears and $\omega_2 = k\omega_1$, the equation above may be simplified to $Q_{t1} - Q_{t2} = PQ\omega_1(1+k)$. This shows that as the gears move from its point of approach to its point of recess it transitions from maximal negative to maximal positive sliding respectively. At point P, the distance PQ is zero, which indicates a pure rolling condition at the pitch point as shown in Figure 3.8. For the gears used in our transmission, the function may be mathematically derived as:

$$R^2 = x^2 + y^2, \qquad \text{Equation 3.5.2}$$

$$x = r(\cos\theta + \theta\sin\theta)\ and\ y = r(\sin\theta - \theta\cos\theta) \qquad \text{Equation 3.5.3}$$

$$\therefore R^2 = r^2(1+\theta^2) \qquad \text{Equation 3.5.4}$$

$$R = r\sqrt{1+\theta^2} \qquad \text{Equation 3.5.5}$$

This then may be used to find the length of PQ, using the cosine law

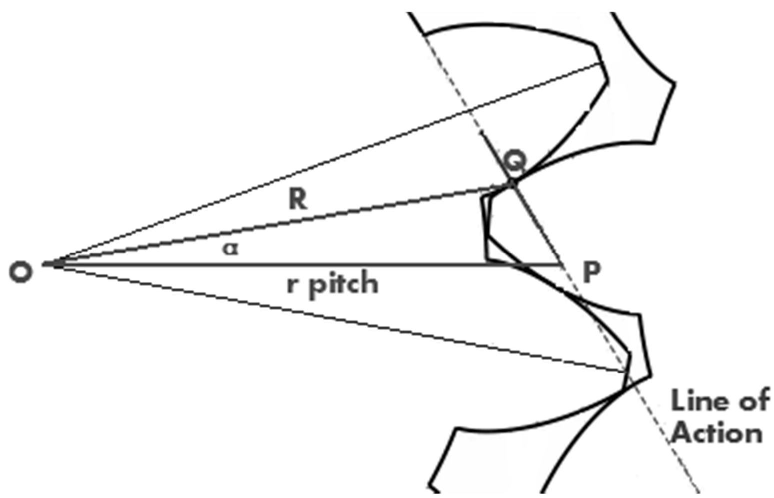

Figure 3.8 Calculating the Length of PQ using cosine law

$$PQ^2 = R^2 + r_{pitch}^2 - 2Rr_{pitch}\cos\alpha, \quad \alpha = \theta - {}^{\pi}/_{20} \qquad \text{Equation 3.5.6}$$

$$PQ = [r^2(1+\theta^2) + r_{pitch}^2 - 2(r\sqrt{1+\theta^2})r_{pitch}\cos\alpha]^{1/2} \qquad \text{Equation 3.5.7}$$

Since r and r_{pitch} are constants, and α is merely a shift of θ, then the only variable in the function is θ. The entire function remains positive because the cosine law cannot produce a negative length. Since the sliding velocity can be negative, based on the relative vectors, the sliding velocity varies from negative to positive as shown in Figure 3.9.

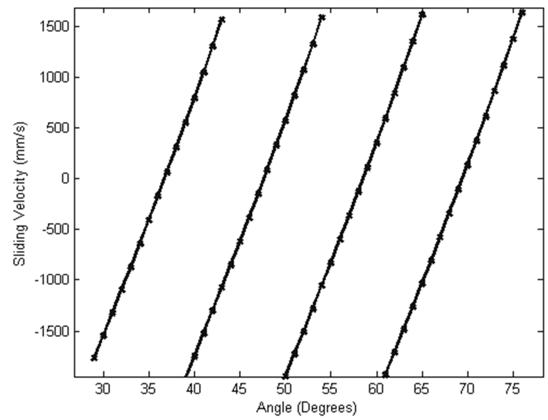

Figure 3.9 Flank Face Relative Sliding Velocity

This is congruent with the theory because ω and k are both fixed values, so the sliding velocity will be a simple multiple of the distance. It was, however, surprising to have the function be so linear, but can be rationalized as a specific property of involutes based on their mathematical design.

Based on the vehicle performance, outlined above, and using its full throttle acceleration as the condition, the sliding velocity of the gear flank face can reach values as high as 2 m/s. Again, this is not the mean value, but is the maximum velocity of the flank face.

3.6. Involute Tooth Profile

The gear tooth profile is designed for each individual function and how it interacts with other gears. Pump gears, bevel gears, and transmission gears all have different tooth profiles. For transmissions, the most important job of the transmission is to transmit power/torque from one gear to another. Involute gears are very effective at this, as they are mathematically designed to maintain a constant pressure angle throughout the contact. Shigley walks through how this tooth is formed [32]. Their mathematical shape is created by making a line of tangent equal to its arc length from its reference. This process is illustrated in Figure 3.10.

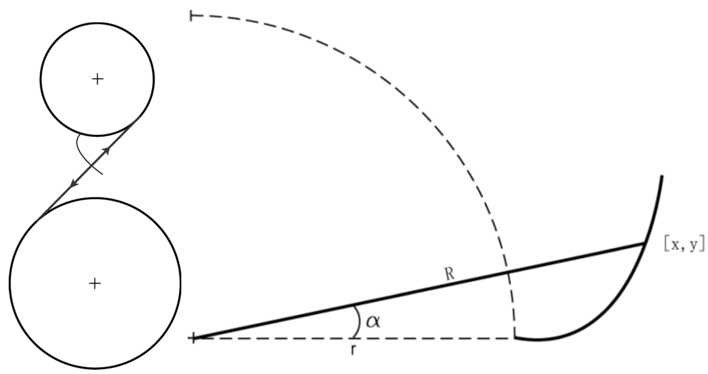

Figure 3.10: Involute Curve

An involute profile may be modeled by the function:

$$x = r\ (\cos\alpha + \alpha\sin\alpha) \qquad \text{Equation 3.6.1}$$

$$y = r\,(\sin\alpha - \alpha\cos\alpha) \qquad \text{Equation 3.6.2}$$

For which the flank radius, R, can be calculated at any given angle with the use of the Pythagorean Theorem.

This specific geometry is designed to ensure that the relative rate of rotation between the gears remains constant and that the point of contact between the two teeth follows a straight path [33]. This path is the line of action, offset from normal by the pressure angle, and tangent to both base circles. While this condition only holds for involute gears, many gears which are of a similar profile will have a similar path. For this reason, it is assumed that the path may be approximated as linear for the gears studied. When two complimentary involutes are in contact, their normal contact is always perpendicular to the direction of motion, and the direction of force remains constant throughout the contact. This makes the free body diagram (FBD) much easier to work with. While not all transmission gear teeth are involute, it is assumed they are for the purposes of this study.

3.7. Contact Pressure

The force analysis is first formed from the FBD of the gear teeth, which is then modified into 2 dimensions to consider the axial forces generated by helical gears.

Hertzian contact theory considers elastic deformation of materials under load, which plays an important role in calculating the observed contact area. In spur gears, the line of contact changes to an elliptical area of contact which is maximal at the center of the tooth. This same concept also translates to helical gears. Through this, the maximal contact pressure found at the center may be calculated as:

$$\sigma_o = \sqrt{\frac{W(1/R_1 + 1/R_2)}{F\pi[(1-v_1^2)/E_1 + (1-v_2^2)/E_2]}} \qquad \text{Equation 1.1.2}$$

The radius of curvature at any given point on the flank face can be calculated. The curvature of the tooth during the greatest amount of loading is what will be used for calculations and testing. This occurs at the pitch point, and is almost exactly the average of the curvature. For the gears in question, this radius of curvature used for calculation is 35mm.

A mathematical model has been formed in Matlab to calculate the contact pressures of the gear teeth. This has been evaluated using physically measured parameters, operating in worst case conditions, to determine the maximal realistic loads the teeth would observe. This exists when both the motor and ICE are running at maximum torque to accelerate the vehicle. During maximum acceleration, the gears are found to experience nearly 2 GPa at the contact line. This is an unexpectedly large value, but it is corroborated by several other researchers studying similar applications [34].

From gear theory, it is understood that the teeth go through smooth loading where the contact load is minimal at engagement and exit, and maximal at pitch point [22,27,35]. Song He demonstrates a similar model in his prediction of dynamic gear forces. While his method considers dynamic conditions, the limits and calculations are the same [36].

Our calculated model illustrates the friction force in Figure 3.11.

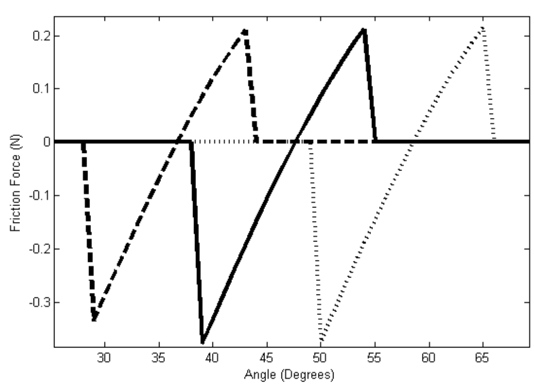

Figure 3.11 Friction Model of Meshing Gear Teeth

Song He's model is similar to the models calculated here. Disparities between his results and those presented here exist because these calculations assume infinite rigidity. The dynamic effects captured by Song He's study is not important for this research because the purpose of the model was only to establish bounds on the operating conditions.

3.8. Temperature

Variations in temperatures can change the mechanical properties of the surfaces, and encourage chemical reactions to occur. Conversely, reduced temperatures have the ability to increase fluid viscosity, which increases the potential losses in power. Clearly, changes in temperature have a significant effect on the performance of the system and coatings. Also, the pressure and friction energy at the center of the point of contact generates localized heat. This temperature is often substantially higher than the measured ambient; so much so, that one is not indicative of the other. With all of this said, temperature was not something that could be measured during preliminary tests of the transmission. Nor was it possible to recreate these ambient temperatures with the chosen tribometer. The only relevant data found was from the MSDS sheet for the Mercon V ATF [37]; which it states that the flash point for the fluid is 177˚C. Many reports comment that a typical transmission operate near 100˚C [37]. Since this temperature is a secondary response to the pressures and speeds that the gears are operating at, it is assumed that by recreating them, the localized temperature will naturally be recreated.

This is a potential source of error in the tests, but is consistent for all of the tested samples. While it may affect the reactivity and performance of the coatings, it would affect each of them equally. Furthermore, these coatings are designed to be inert and to withstand temperatures above 200˚C, so the likelihood of them not performing as designed while surrounded by a heated fluid is doubtful.

3.9. Summary

From the discussion above it is established that the most extreme operating condition which may cause gear failure is full throttle acceleration. An involute gear is a good design of gear teeth because its shape allows for normal forces to travel constantly in the same direction. For upcoming tribology tests, the samples will be made from 8620 steel and will experience velocities as high as 2 m/s and contact pressures reaching 2 GPa to mimic the calculated operating conditions. Ambient temperature and other secondary conditions which cannot be simulated were held constant for all of the tests. Since no changes to the ambient were noticed, any error caused by it is assumed to be consistent throughout all tests.

Chapter 4. Other Factors for Coating Selection

With friction technologies advancing to such a high degree, it is now important to shift the focus to the environmental implications of the chemicals and processes which are used to achieve these results. Using hazardous chemicals in the mass production of gears can lead to hazardous waste or pollution created which can have negative effects to the surrounding environment. In each of the stages of a coating's life-cycle (manufacturing, operation, recycling/disposal), there exist opportunities to minimize the impacts these technologies have on the surrounding environment. A key threshold for each of these stages is to avoid shifting from non-hazardous to hazardous waste. The goal in every stage is to advance the technologies towards environmentally sustainability and increased recyclability. If a coating application is found to have great friction reduction properties, but is deemed hazardous, then it no longer qualifies as a viable solution.

Current efforts in coating technology are to reduce or eliminate the use of sulphur based compounds. This is because of the hazardous fumes and burn-off which is formed during its breakdown and end of life. Sulphur is commonly used as an extreme pressure additive in lubricants and solid surface coatings, as well as in metal cutting to improve the machinability of the stock material. If non-sulfur-based chemicals can be found to achieve the same performance, this would very well be a step in the positive direction, which may also be extended to other applications in which sulphur is the conventional solution.

4.1.1. Environmental Considerations - Processing

The processing and application of the coating can form by-products which have an equal importance to the environmental impact. Before a coating can be chosen for full scale production, every aspect of its production must be evaluated for environmental concerns. This information was not available for this study, but is an important factor to consider before it can be implemented.

In order for the application of the coating to be viable for OEM's it must also be financially worthwhile. The cost for applying a coating has to provide a reasonable return to the producer. Furthermore, it must be easy to implement in the current production process. The problem with PVD's is that it is a batch manufacturing process, while the rest of gear production lines are part-by-part. This would create a discontinuity to the production, and may cause conflicts in the manufacturing process and may make implementation difficult.

4.1.2. Environmental Considerations - Operation

Even minor improvements in the friction performance of the gear teeth have the potential to generate substantial fuel savings over the running-life of the vehicle. This is the best opportunity for surface treatments to have a positive effect on the vehicle's performance, fuel savings and environmental impact.

On the other hand, due to the high temperatures and various chemicals present in the transmission, there is the chance for these coatings to wear and chemically react with the oils or additives during the vehicle's lifetime. Having a chemical reaction take place raises the question of whether a hazardous chemical may be formed from the reaction. The coatings in question are selected based on their wear resistance, and low friction coefficient. These types of performance additives are designed to be inert. For this reason, there is little concern of any chemical reaction taking place between the coating and any materials or substances found within the transmission. Nor is there any concern of any hazardous material being formed during the running life of the transmission as a result of a coating application.

4.1.3. Environmental Considerations - Disposal /Recycling

The information provided in the following section has been gathered from the posted resources as well as from discussions with Dr. David DuBois and Dr. Edmund Rodrigues [38]. Dr.'s DuBois and Rodrigues are experienced environmental engineers who specialize in the classification and disposal of waste within Ontario.

In the disposal of used automotive parts, cars are stripped and sold at junk yards or melted down and recycled. The aim is that at the end of life of the transmission, there will be little to no waste. Disposal of materials is both wasteful and costly. Disposal cost is dictated by the classification of waste, where it needs to be disposed of, and the volume of it. Waste is classified through Regulation 347 from the Ontario Ministry of Environment as either hazardous or non-hazardous waste. Within the realm of hazardous waste, material can be categorized into seven further categories. Essentially, the higher the class of hazard, the more costly it is to dispose of. With any of the surface treatments under investigation, all options should maintain or improve the environmental impact observed.

Currently, the transmission case and gears are melted down for recycling. Transmission fluids are recycled and made into other industrial oils, but this process still produces hazardous sludge during its reformation. If it were possible to use other additives and chemicals helped it produce less waste, or downgrade its classification, this would have significant benefits to the producer and to the environment. This is currently being attempted by Mr. Mark Miller at Terresolve [21]. They are trying to replace the current sulfur based additives, with non-hazardous substances, while achieving the same level of performance. Terresolve is also exploring using different, renewable base oils in which to create a transmission fluid from.

Chapter 5. Coating Selection

The first step in attempting to reduce friction in the transmission is to understand the theory of friction and how it applies to gear motion. Losses are generated by gear tooth interaction, bearing losses, lubricant churning (fluid friction). The total losses of the power transmitted, is due to a summation of all the losses outlined above. Of which, this study focuses solely on the gear tooth flank face.

Several coatings have been investigated to see which has the best friction and wear characteristics. This was examined using a pin-on-disc tribometer. This form of testing was done to ensure unbiased results by performing them under controlled operating conditions.

Custom specialized coatings would be an option but it is outside the scope of this study.

5.1. Investigated Coatings

Six sets of pins and coupons were custom fabricated for testing to recreate the calculated contact pressures. Each set comprised of two pins and one coupon. One set was left case-hardened but uncoated to act as a benchmark for testing. It was noted previously that all of the gears carried consistent mechanical properties; which is to say, they were all made from the same material, treated with the same hardening process and had the same surface roughness. The decision to apply coatings to both the pins and coupons was an extension of this observation. Coating both interfaces was intentionally done in order to maintain this mating of similar surfaces. Furthermore, it was a concern that deciding to coat only the pin or only the coupon would have an effect on the performance of the samples.

Five coatings were selected for testing on the remaining samples, which are outlined below:

5.1.1. Tungsten Disulfide, WS_2

Tungsten Disulfide (WS_2) and Molybdenum Disulfide (MoS_2) are similar dry lubricants and have been in use for many years now and widely recognized in bearing, automotive, tooling, molding and aerospace applications. For a long time, MoS_2 was more economical but, as of late, has been increasing in cost to the point where both compounds are of comparable prices. With WS_2 performing superior to MoS_2, and now also being a similar cost, it is more suitable to go with the slightly more expensive coating. It must also be noted that the properties of both of the compounds are very similar, and only vary in extreme conditions, which go well beyond the limits of our normal operating conditions. From this, both components are almost indistinguishable and are equally suitable for this study.

Tungsten disulfide is commonly used because of its performance under high pressures, resilience to temperatures below 650°C and exceptional friction coefficient. It has a hardness of 30HRc and a thickness of 0.5 µm. The problem with its extensive use arises because of its sulfur content, as described earlier. This is being tested as an industrial benchmark.

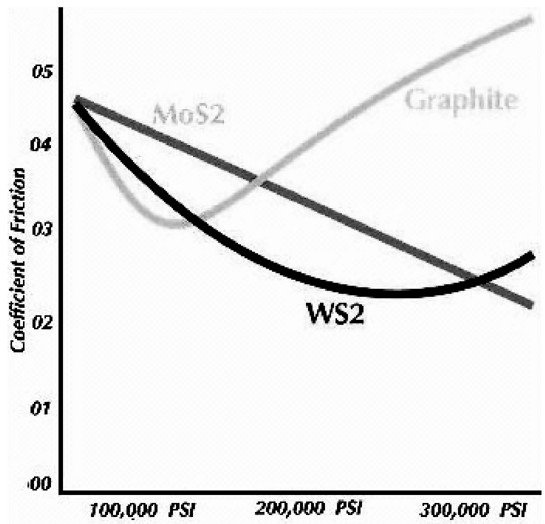

Figure 5.1 Brycoat Performance Graph [taken from 39]

This graph, provided by BryCoat [39], illustrates the ideal operating pressures for 3 different coatings for minimal friction. This shows the potential friction values to expect from WS_2. It claims to have low hardness and good interaction with petroleum based lubricants. This graph also shows MoS_2 and WS_2 to be more likely than graphite to be our choice coating. All of these factors suggest that this will be a high performing sample in upcoming experiments. Further information about this coating may be found on the BryCoat's website.

5.1.2. Chromium Nitride, CrN

Chromium nitride is a surface coating typically applied to metal cutting tools and equipment used in sterile operations. BryCoat claims it has good adhesion and high durability to metallic surfaces. It has a hardness of 82HRc and coating thickness of 4 µm which suggests it may be a good option for gear applications. It is an inert, non-toxic material which uses environmentally friendly processes for production [40]. One concern with this coating is that the coated component needs to be heated to

375°C during the deposition process. Such a high temperature is capable of nullifying the previous case hardening of the pins for this testing and for the gears in final application. Weakening the substrate may have negative effects on the performance of this sample under load. Although its measured coefficient is relatively high, it may still be a viable candidate to act as a base coating to then apply a softer lubricious coating over top of.

5.1.3. Tungsten Carbide - *Balinit C WC/C (a-C:H:W)*

Developed by Oerlikon Balzers, this coating is designed specifically to reduce abrasive wear in dry sliding conditions in order to improve performance in gear and ball bearing applications with high surface pressure levels. Its high hardness and low CoF may also allow for softer / cheaper substrate steels to be used. Balzers notes its biocompatibility and quality performance for loaded gears and bearing applications, which suggests this to be a good candidate for testing.

5.1.4. Balinit DLC Star - CrN + a-C:H

Diamond Like Carbon (DLC) coatings tend to be very hard and have good adhesion to their substrates, but are very brittle. This explains why it is necessary to apply a lubricious coating over top of it to protect it from wear, and improve the friction properties [41]. This gives the balance between high hardness and low shear strength desired for friction reduction.

This modified coating has been designed to have an increased hardness surface layer to enhance wear performance of a cyclically loaded component and minimize fatigue. It uses chromium nitride as the base layer with a carbon based outer layer surface which is designed to provide lubrication. The inclusion of the hydrogenated carbon aids in the coatings retention of the lubricant which may further improve its tribological performance.

5.1.5. Surface Texturing

The super-finished set is unique to the coating samples because it is a surface treatment rather than a chemical coating. Li Xiao shows, in his thesis [42], that the smoother the surface the better the frictional performance, but Josh Tovey shows, in his thesis, how textures help retain the lubricant in the sliding zone [43,44,45,46,47,48]. Tovey claims that there is an optimized roughness to consider. In

Tovey's case, the texture is present to allow coolant to remain in the interface during a machining operation. Also, his experiment operated on the cutting chip material whose real contact area is close to the apparent [49].

To study surface finish pins were sent to the Metal Improvements Company (MIC) with the same roughness as the other samples. The samples underwent a controlled shotpeening process with ceramic shot at a controlled velocity. The impact from each shot particle forms a localized micro-hardness which forms a layer of compressive residual stress as shown in Figure 5.2.

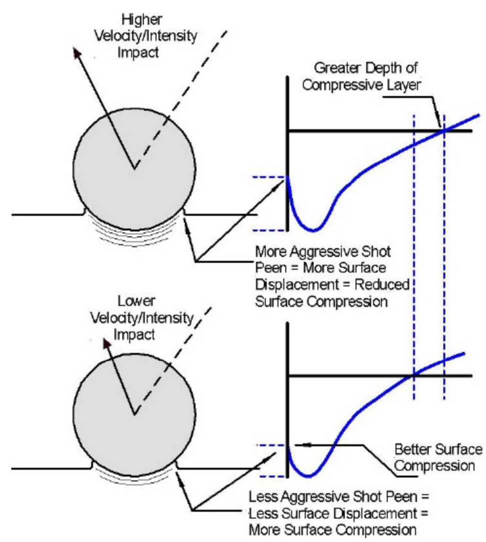

Figure 5.2 Residual Stress Caused by Shot Peening [taken from 50]

The depth and value of the stress can be controlled through the material, size and speed of the shot particles. After this processing step, the samples are then honed using an acid solution. The goal of this chemical erosion is to eliminate peak asperities while preserving the valleys necessary for fluid retention as shown in Figure 5.3.

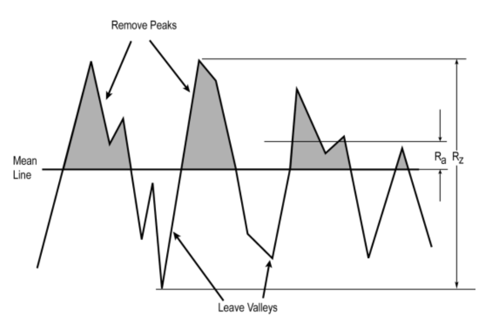

Figure 5.3 C.A.S.E Process Polishing [adapted from 51]

This process is suggested to reduce the frictional effects because it minimizes the asperity contacts while retaining fluid lubricants between the surfaces. This process is commercially referred to as C.A.S.E processing at MIC, but will be referred to as 'superfinished' for the remainder of the document.

5.2. Cost

The coatings listed above have been chosen to be applied on the samples. This will play a role in the consideration of the ideal coating after the friction tests are tabulated. The estimated values of the coatings applied are as follows (above the cost for material and carburizing):

Table 5.1: Cost Breakdown of Surface Engineering Technology Services

WS_2	$3.25 per pin and $18.75 per coupon. Totaling **$35.00** (Min order cost is $100)
CrN	$6.40 per pin and $24.20 per coupon. Totaling **$56.20** (Min order cost is $100)
Balinit C	$12.05 per pin and $46.77 per coupon. Totaling **$107.02**
Balinit DLC Star	$24.11 per pin and $93.53 per coupon. Totaling **$214.08**
C.A.S.E Processing	Total **$800.00**

The values presented above are a record of the cost for the services applied to the test samples for the research. This record is designed to offer a cost comparison of treatment value. However, these evaluations are not indicative of the cost per part estimated for large volume orders like those expected to be carried out by large automotive manufacturers. Clearly CASE Processing is much greater in cost than the other applications. However under high volume orders, MIC claims to have costs competitive to other surface engineering applications. In large scale applications, the cost for materials is only one small aspect of the cost evaluation. Other considerations like licencing, equipment, and integratability are significant factors to evaluate in order for the surface treatment to be viable and worthwhile for manufacturers. This level of investigation into cost analysis is beyond the scope of this research.

5.3. Prospective Coatings

Among the coatings of interest for study, only five were selected. Seung Min Yeo, from the University of Illinois has performed similar experiments using other coatings from Dupont, and has found exceptional performance from PTFE/MoS_2 and PTFE/Pyrrolidone2 [52]. These, as well as hexagonal boron nitride and titanium-nitride would be coatings of interest to test in the future.

5.3.1. Hexagonal Boron Nitride, h-BN

This inorganic material is synthesized from boric oxide. It is produced to have superior characteristics than graphite. Cubic boron nitride has similar properties to diamond but is not considered for this study because of its poor lubricating properties. h-BN is a soft white powder which is applied via electro-deposition. Four ball wear tests show that h-BN has one of the lowest coefficients of friction of common solid state coatings [53]. Due to its mechanical properties, it is used in a wide range of applications from mold releases to aeronautics to glass making. Hexagonal boron nitride is recognized as holding many of the desired properties of our conditions including: chemical inertness, high thermal stability and excellent lubricity. More study must be continued to understand its environmental impact for later tests.

5.3.2. Teflon, PTFE

Teflon coatings have been noted by Dupont, to have a low CoF, chemical inertness, and heat resistance. All of these qualities listed are necessary to ensure a reduction in friction, and an improvement in the wear of the gears. Dupont provides several different types of Teflon coatings for various applications [54,55,56]. Seung Min Yeo has explored modified Teflon coatings for similar applications and has achieved promising results from similar sliding tests. Particular coatings of note include PTFE/MoS_2 PTFE/Pyrrolidone2 and PTFE/PEEK. These coatings could not be secured in the time frame of this study, but it is recommended for these coatings to be included in future tests.

5.3.3. Tungsten Disulfide, WS_2

Tungsten disulfide has many desirable propertied for gear tooth sliding [57]. It is currently used in various automotive applications, such as: bearings, cams, power transmission components, oil additives, etc. However, its MSDS [58] sheet states that it is highly acidic, and ecologically damaging if not disposed of properly. Since WS2 is one of the best low friction coatings currently available, its application will be limited to only the sliding environments which are most severe.

Chapter 6. Testing Methods

6.1. Considered Tribometer Testing Methods

ASTM (American Society for Testing and Materials) offers various standardized tests to test aspects of gears, coatings, etc. Each test is designed to focus specifically on one aspect related to friction or wear. The following are prevalent options commonly used for wear and friction testing. This is by no means an exhaustive list, but a list of a few testing apparatuses considered for use.

6.1.1. Four-ball

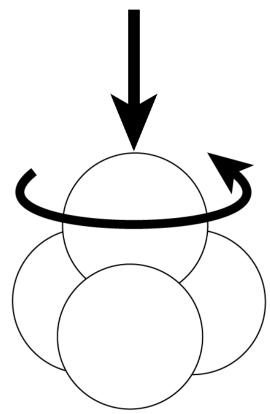

Figure 6.1 Four Ball Wear Tester

A four-ball tester as outlined in ASTM D5183, D4172, D278 and others is shown in Figure 6.1. It is a simple method of loading a single rotating ball on top of three other identical balls grouped together below it. This is an effective method at measuring wear on point contacts. The four-ball tested is favored for extreme pressure sliding in wet and dry conditions. While this is a great way to compare performance of different coatings against each other, it however is not appropriate for simulating a gear tooth interaction because it does not simulate the sliding environment of the gears.

6.1.2. FZG

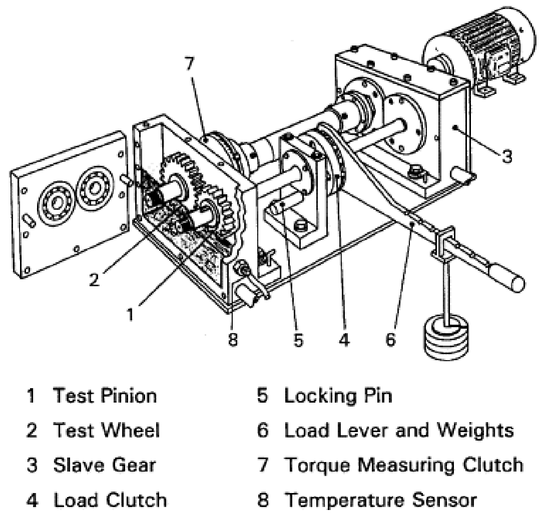

Figure 6.2 FZG Tribometer

This German designed testing apparatus, shown in Figure 6.2, is widely accepted in Europe as an effective testing apparatus for many gear applications. It involves two parallel shafts connected via gears at both ends of the shafts. They are driven by an electric motor connected at the middle. The gears are partially dipped in an oil pool which allows them to lap up necessary lubricating fluid. This is an effective way to identify fault modes (scuffing load capacity, occurrence of micropitting) [59], performance of fluids and performance of gears under specific conditions. The problem with this test is that the FZG machine only allows one size of gears onto the shafts. This limits the versatility of the machine for testing different gear sizes and materials.

6.1.3. Pin on Vee-Block

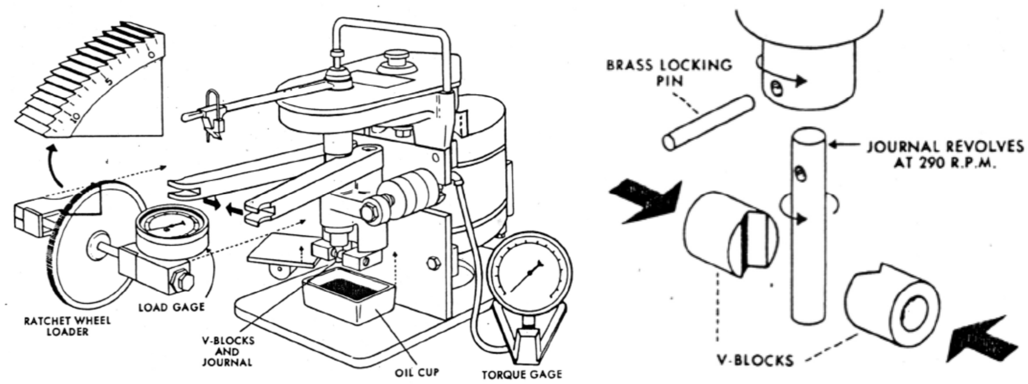

Figure 6.3 Falex Tribometer

The pin-on-vee-block tribometer, shown in Figure 6.3, is made by Falex [60], and is available for use in the MMRI. Our model is not currently linked with electronic sensors and so has limited capabilities for data collection. The design of this machine places a rotating pin between two clamped v-blocks which forms four contact points (two per block). During a test, a ratchet draws in the clamping arms so that the clamping pressure grows incrementally until seizure occurs. This tester has been used for experiments relating to Extreme Pressure lubricants and endurance limits of solid film lubricants, in accordance to ASTM D2625, D2670 and D3233. This test is good to analyze a coating's performance under high loads and is good at forming repeatable wear but its design does not sufficiently simulate the gear tooth sliding experience.

6.1.4. Reciprocating (chosen option)

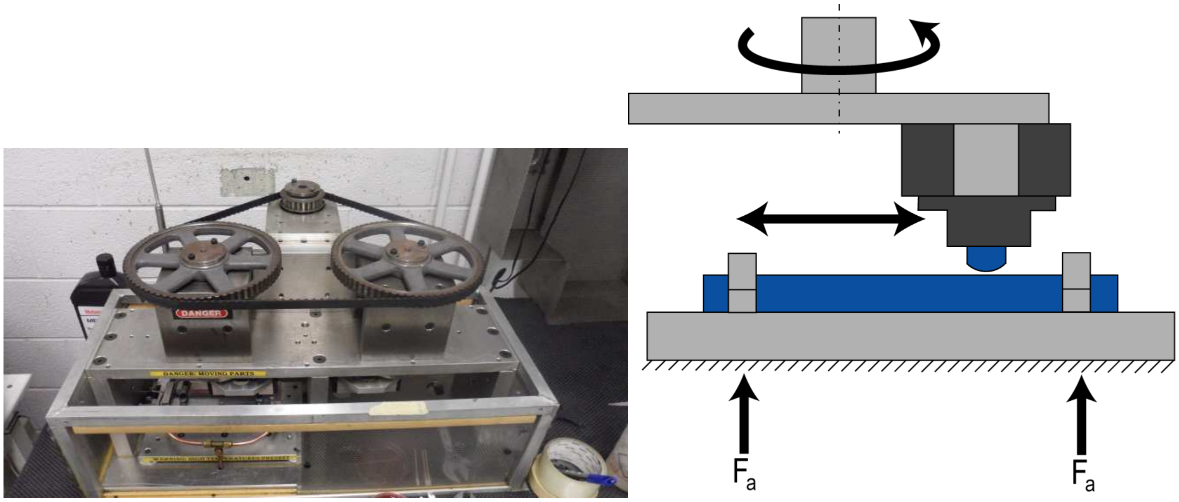

Figure 6.4 Windsor Reciprocating Tribometer

The reciprocating tribometer, shown in Figure 6.4, is a simple design which allows a pin contact to slide against a fixed plate. This home-build design at the University of Windsor was developed by a graduate student nearly a decade ago. This setup allows for the pin to be connected to an eccentric crank arm which rotates at a constant angular velocity. This produces a reciprocating 1-dimensional action which follows a sinusoidal velocity curve. The load is attached by a statically weighted lever below the table which applies the gravitational force upward on the plate. The tribometer is still used regularly by Dr. Alpas at the University of Windsor to teach undergraduate students the fundamentals of tribology by conducting simple sliding tests which simulate piston-cylinder sliding in a combustion engine.

While Section 3.7 illustrates the contact pressure as a gradual growth, until maximum at pitch point, and gradual decline until exit, this tribometer is only able to apply a fixed load. To resolve this disparity, multi-load tests were designed to capture many points on the curve, as discussed in section 8.1. It is assumed that values in between the tested loads may be interpolated.

The samples here must be custom made in order to fit into the apparatus, and have the appropriate dimensions. A Zygo Newview 5000 microscope measured the flank surface roughness to be between 20 and 50nm (Ra). These parts were fabricated from AISI 8620, case-hardened to 63 HRc and ground to a surface roughness of 33nm Ra to match the gears. The curvature of the pin head was machined on the Boehringer VDF-180CM CNC lathe to have a tip radius of 19 mm. This was to generate the equivalent contact between a pin on plate as observed between two flanks. Coupons were machined to be 12mm x 12mm x 152mm and ground to a surface roughness of 350nm.

Of the testing apparatuses discussed, the reciprocating tribometer has been selected for use because of its ability to simulate the sliding velocities for a range of contact loads. This is the best available design which mimics the gear tooth sliding interaction.

Chapter 7. Preliminary Testing

7.1. Load Sensor Calibration

The friction force is captured using an Omega LCDA-25 load sensor [61]. This is connected to the base, which is free to move laterally, so it can measure compressive and tensile forces. The load sensor was calibrated using known weights statically loaded on the system. The setup is shown in Figure 7.1:

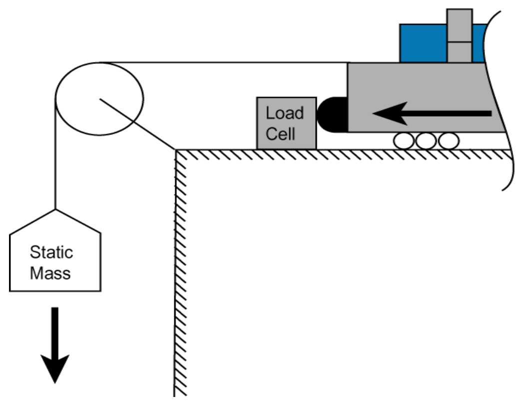

Figure 7.1 Load Sensor Setup

This test was performed each day to ensure accurate calibration. All calibration tests demonstrated a linear relationship, but differed slightly from day to day. Each day's calibration values are used for tests performed on their corresponding day to convert the voltage signal received from the load sensor into force values. The data collected is illustrated in Figure 7.2 and their calibration curve is formed in Figure 7.3.

Results:

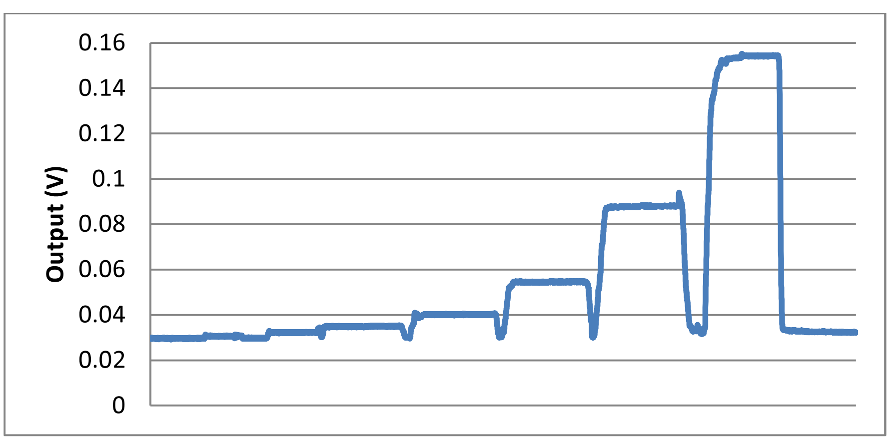

Figure 7.2 Load Cell Calibration with Known Weights

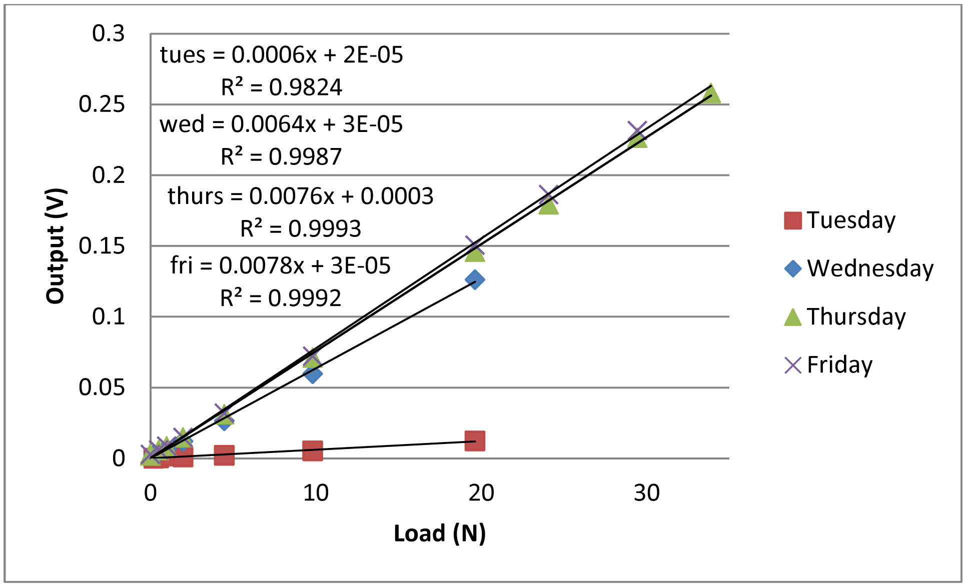

Figure 7.3 Daily Load Cell Calibration

Tuesday's calibration curve differs from the rest of the days values by an order of magnitude. Nevertheless, diligent process was carried out to maintain consistency from day to day. Careful back-calculation of Tuesday's tribometer indicate that the force values are consistent with all other data collected on other days. For this reason, Tuesday's data was not omitted from the data set.

7.2. Drift

Two tests were conducted to analyze the potential of drift in the sensor. Each test was performed for 120 seconds, which is 100% longer than the duration of any of the friction tests. The first test was performed with no load, and the 2nd was done with a 2kg static load. Both show a 1% drift, which may be neglected, as it is within the limits of the sensor's error.

Error = max(value) – min(value),

Drift = avg(t=1 sec) – avg(t=120 sec).

Error (no load) = 0.000679253, Drift(no load) = 7.7625E-05

Error (2kg) = 0.0427, Drift (2kg) = 9.52083E-05

Results of the setup testing is shown in Figures 7.4 and 7.5:

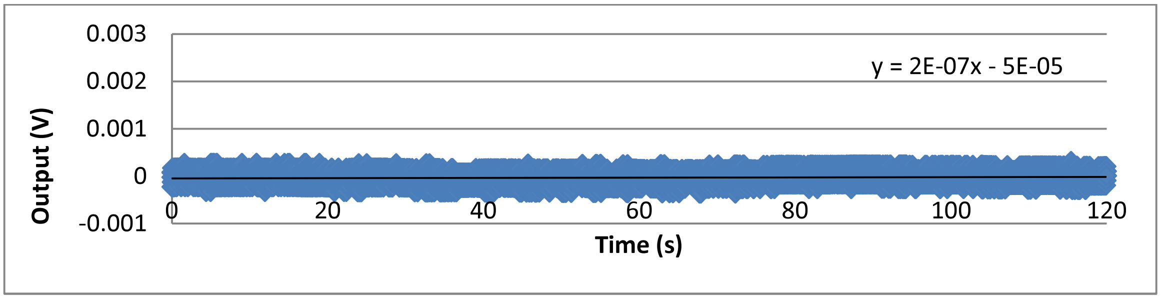

Figure 7.4 Drift Test under No Load

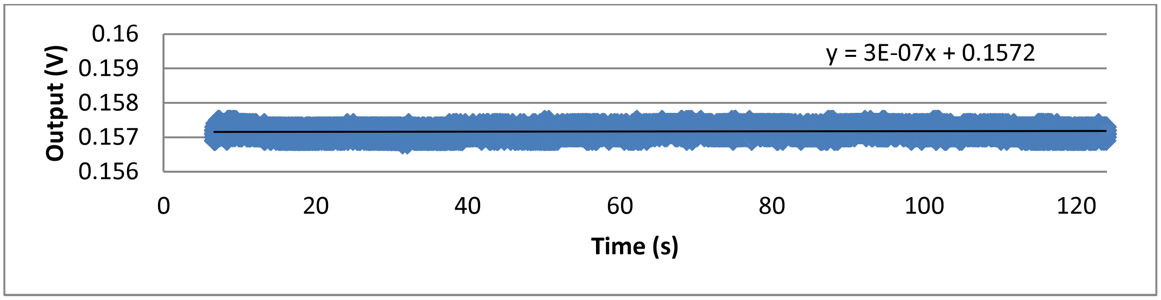

Figure 7.5 Sensor Drift Test under 2kg Static Load

7.3. Noise

With the machine off, and the sensor running, data was collected in order to measure the inherent noise of the sensor. This was performed multiple times with no load and a 2kg hanging load. A Fast Fourier Transform (FFT) was conducted to see which frequencies where dominant in the system noise. Noise test results show a steady signal within the error bounds. From this study, it is decided that no filter was necessary for the signal.

7.4. Sources of Error in Reciprocating Tribometer

The tribometer in Windsor was chosen because it reasonably simulates the sliding interaction of a gear flank face. However, its operation still has faults inherent in its design.

- Alignment: If the reciprocating track and the plate are not perfectly parallel, then the plate will be driven downwards as the pin travels to the high side of the plate (left or right extremity). This will clearly have an impact on the loading as the momentum of the bottom table will have a dynamic motion to the testing. Inertia of the sliding block will add to the friction results because it is changing the observed load (F= ma + kx). This can be seen visually by the bouncing of the weights during testing. This should also be seen by variances in the peaks and troughs of the output as well as the FFT of the signal. Major spikes in the FFT are expected to be found in places which correlate to the reciprocating action of the pin (~3Hz), low frequency beats in the samples due to the motor (~1 or 0.2 Hz) and the weights bouncing (~5Hz) would be seen if setup problems were present.

- Velocity: The motion of the reciprocator does effectively operate through the appropriate range of velocities. However, it does not accurately mimic the near zero rolling action which happens at the pitch point. This is the position in which the largest friction force is observed, and encourages extreme wear at this point because there is no lubricant to separate the surfaces. This is in line with fluid theory illustrated through the Stribeck curve, but may not be an accurate representation of a gear.
- Motor: The relative sliding velocity of the gear flank faces were initially presumed to be sinusoidal. But through Matlab simulation, it is now known to be almost perfectly linear. This creates an error in the simulation of the sliding interface because the tribometer generates a sinusoidal motion.
- Sensor: As shown from sensor tests, there is a degree of noise which is observed from the sensor. There is little or no drift, but there is hysteresis present at the reversal which will misalign the data with the true position and velocity. This is also seen because the absolute value of the peak is not equal to the absolute value of the trough.

These tests establish the abilities of the apparatus and sensors available. This is important for the understanding and design of the experiments to produce meaningful results. It is also important in order to accurately analyze the results collected. Knowing the limitations of the machine and sensors prevents any misinterpretation of the data.

Chapter 8. Results and Analysis

It was first necessary to conduct preliminary investigations in order to determine what a reasonable testing range would be; both for the validity of the test as well as to generate results which would indicate which coating performed the best.

Since friction is generally independent of sliding speed, if a reciprocating action were to be conducted under dry conditions, the friction force graph would ideally, assuming an infinitely rigid setup, look like a square wave as shown in Figure 8.1. The friction would simply resist the movement with a constant force proportional to the load.

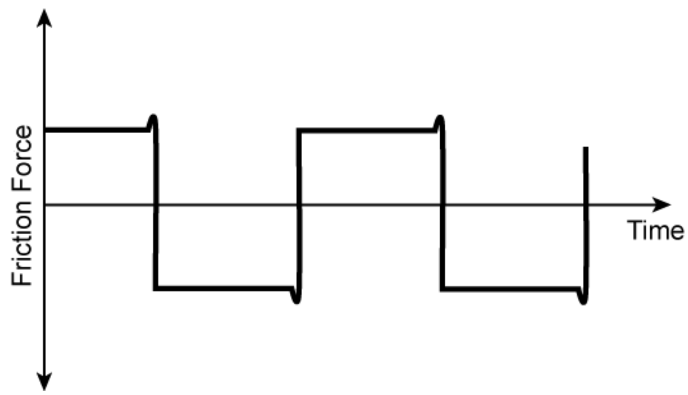

Figure 8.1 Ideal Friction Step Function

A small spike in friction can be seen as the object changes direction because of the momentary zero velocity. This engages the static CoF instead of the kinetic CoF.

Since the tests were run in lubricated conditions, the sliding interaction is more complex than dry sliding. As discussed in Section 2.1.1, when the velocity is sufficiently high, the lubricating fluid is able to generate a boundary layer between the surfaces which then brings the fluid viscosity as the dominant variable in friction. What can be seen in Figure 8.2, is how there is a smooth change in friction as the object slows down. This is because of the fluid still supporting the surface sliding. Yet when the object changes direction, there is a sudden change in force. Even though the velocity profile is symmetric, there is very little fluid between the contacts, which thus encourages stick-slip sliding and static friction until the velocity is sufficiently large.

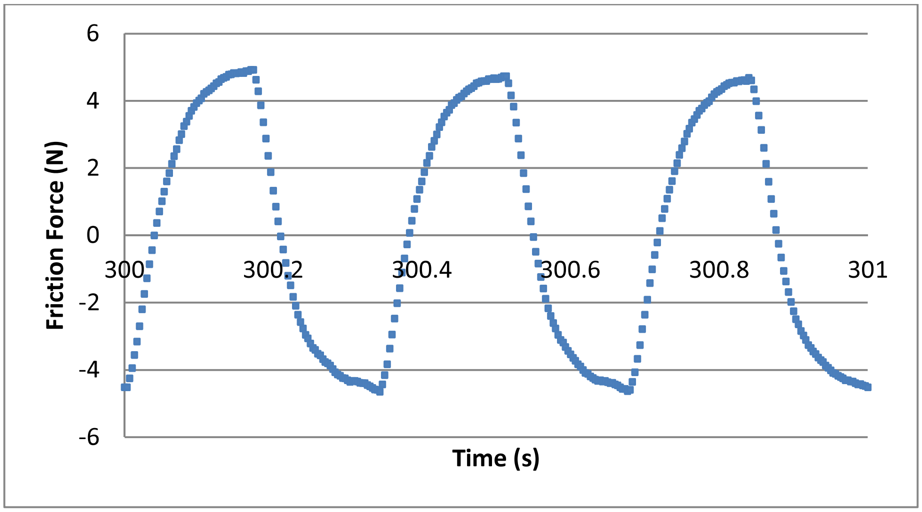

Figure 8.2 Friction Cycle during Reciprocating Motion

But the goal of this friction testing is to determine which coating has the lowest CoF. Therefore, only the region where the coatings are in contact is of concern. When the surfaces are sliding at a low velocity there is limited fluid present to influence the motion. It is during this time that the coefficient of friction is driven by the coating itself. Therefore, the coating CoF is measured as the maximum values from each cycle.

From the friction vs. time plot presented in Figure 8.2 which is a measurement of the frictional resistance observed for the sample prepared with CrN. This shape is common among all of the samples. Let x = 0 represent the home position of the pin at the left most side of the coupon, and x = 1 represent the pin at the right most side of the coupon. The graph starts at x = 0 and begins to accelerate in the positive direction. As the pin approaches x = 1, it begins to decelerate. Near x = 1, the pin is moving at a low, positive velocity and is receiving minimal aid from the lubricant. During the early motion in the opposing direction, the pin then teeters between static and kinetic friction, and causes a noisy signal that was described previously by Booser. When the pin reaches x = 1, it has reached zero velocity and is acting in static friction. As it begins to make its change in direction, the resistance increases until a critical point in which the static friction is overcome and sliding can resume. As such, this is the distinct point which is used as the peak frictional force and is the value to which all coatings will be compared. This data was collected by identifying the maximum friction value observed during each period.

To each data point plotted in Figure 8.3 is obtained based on the maximum frictional forces observed during each test. The mean, variance and standard deviation of these maximal values were calculated to generate appropriate error bars for the graphs. In all instances, the magnitude of the error bars calculated was nearly two orders of magnitude less than the friction values. Therefore, no error bars were included.

8.1. Multi Load Test

The multi-load tests were conducted to observe the performance of each coating under various loads, with wet conditions. The aim of this was to observe if the CoF behaved linearly with respect to the load. Each test lasted 1000 cycles and then was repeated with increasing loads (55, 90, 126, 162, 197, 287, 376, 465 N) on the same wear track. The wear track was inspected after each test to ensure the integrity of the surface. Tests were continued until all loads were tested or until excessive noise from the apparatus was observed. When the motor experienced excessive resistance it was difficult for it to maintain a steady motion. This meant that the sliding motion was not consistent and would invalidate the friction data collected. This data was then not used. An example is illustrated in Figure 8.3 by a gray region were data is rejected.

Unfortunately, it was not possible to monitor the wear rate. Instead, a measure of the wear area of the pin head was measured after all loads were applied.

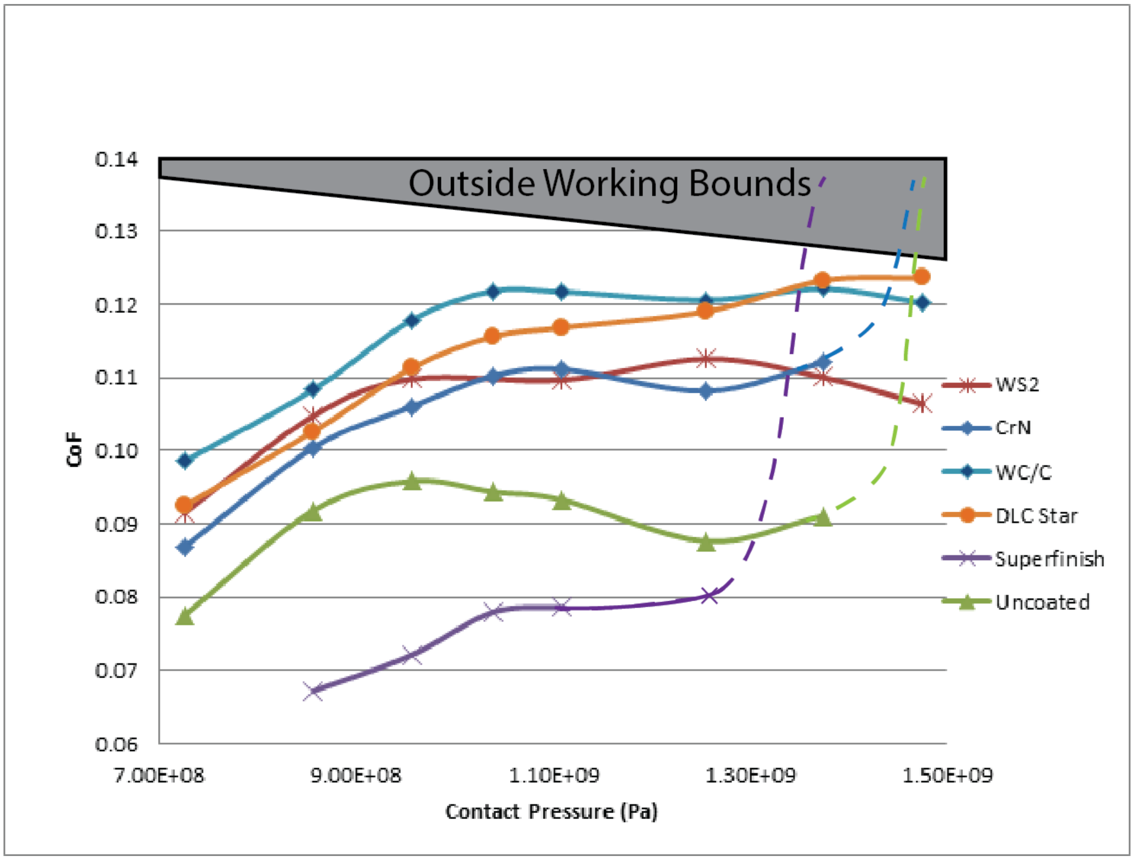

Figure 8.3 Friction Performance of all Coatings Under Increasing Contact Pressure[2]

What is clear from Figure 8.3 is that the superfinished samples and the uncoated specimens performed the best at low loads, but were unable to perform effectively in the higher load ranges. Data from the superfinished tests above 1.40 GPa were invalid, because the resistive load was too great for the motor to overcome, and the test was stopped short. As such, the values for the higher loads were shown to trend into the inoperable region of the tribometer to illustrate the sudden increase in friction. This is very problematic because the loads tested here are not as great as the maximum loads the transmission can experience during acceleration.

It should also be noted that, while the WS_2 coating did not show greater performance than the other coated samples, there is a trend in its performance which suggests that the friction may continue to decrease with higher loads. It is possible that these tests were not loading the WS_2 sufficiently to illustrate its superior performance. Higher loads were not carried out because of the limitations of the reciprocating tribometer to collect reliable data above the contact loads applied. Further study is recommended to see how this coating may perform beyond 1.50 GPa.

[2] Please note that the contact pressure is not entirely accurate, as the contact area changes with load as well as wear.

Considering the good frictional performance of the superfinished sample, and the loading capacity of the WS2 samples, it may be useful to try applying both processes to the samples for testing. This may allow the good qualities of both of the samples for sliding to be utilized.

The non-linear performance of the coating shown in Figure 8.4 could be because of the behavior of the coating, or wearing through the coating, and now changing the friction contact. This nonlinear performance was displayed with all of the coated samples.

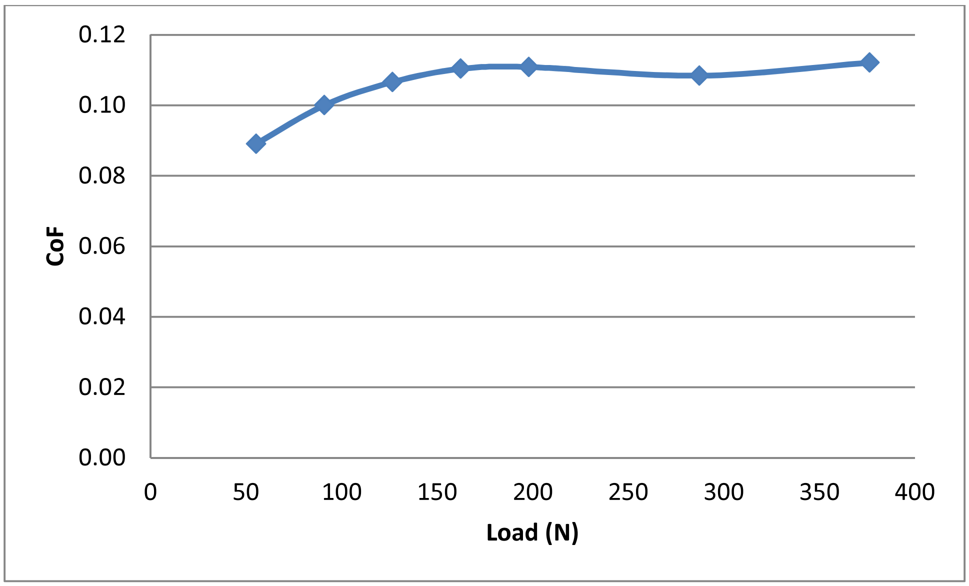

Figure 8.4 Non-Linear coating behaviour of CrN Coating Undergoing Increasing Load

8.2. Long Term Test

The long term test was designed to replicate steady state driving conditions for the Ford vehicle so as to observe how each coating behaves over an extended period of time. Similar to highway driving, the operating load was not severe (168 N), but the sliding velocity was high (250 RPM corresponds to 1.31 m/s). The test was run for 6000 cycles (1200m) and observed at regular intervals to monitor the wear of the samples, to make sure wear was occurring, but not failing, and to reapply lubricant. All samples were clamped and cleaned with ethanol to remove any contaminants during handling. All tests were lubricated by Mercon V ATF, which is the lubricant used in the Ford Escape hybrid vehicle.

In all cases, the friction was initially high, but quickly reduced to a stable value which continued for the length of the test. This shows that the samples did pass through the break-in condition which is illustrated in Figure 8.4 Non-Linear coating behaviour of CrN Coating Undergoing Increasing Load.

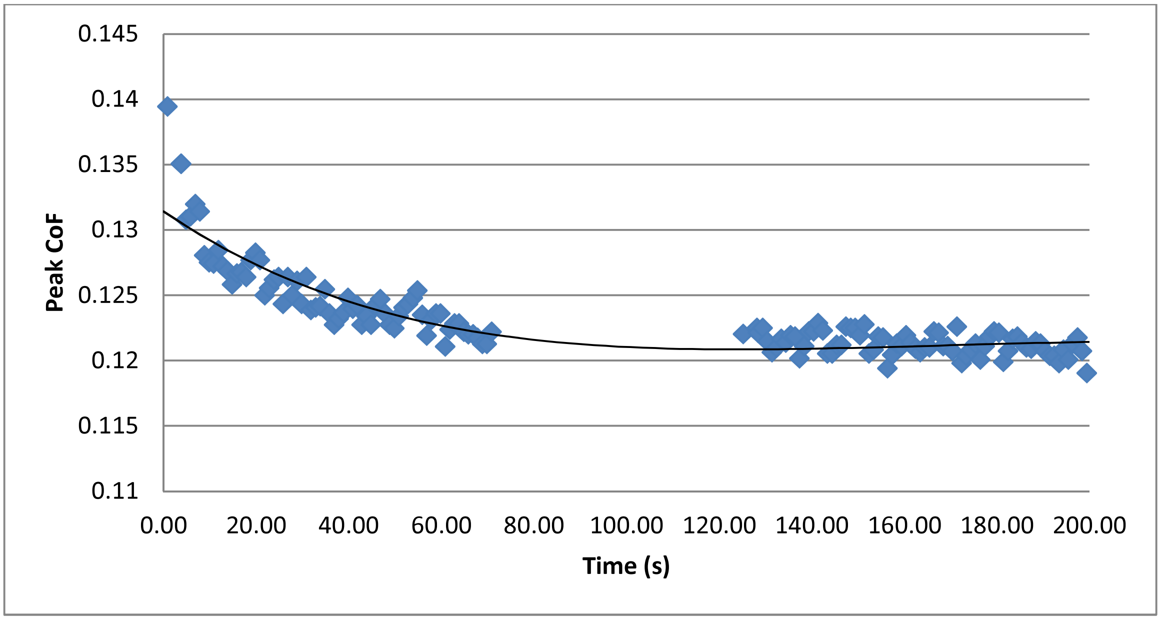

Figure 8.5 Break In

Figure 8.5 and Figure 8.6 illustrates the break-in period which is observed on the samples and also shows the time it took to reach steady state.

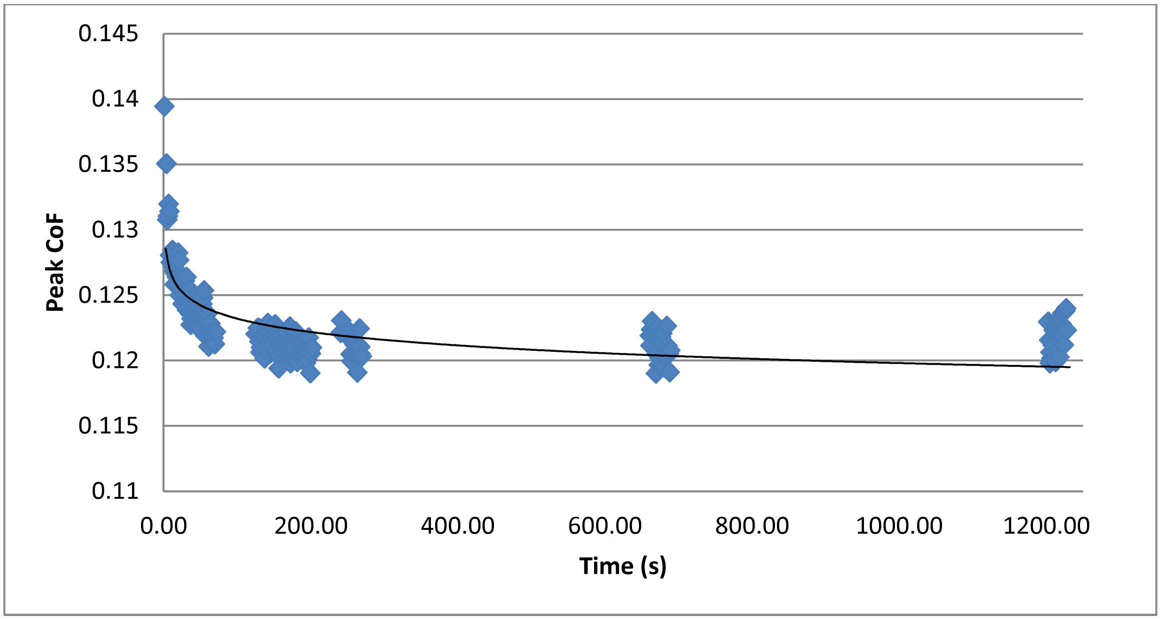

Figure 8.6 Full Test

The Figure 8.7 is a summary of the results collected from the long term tests.

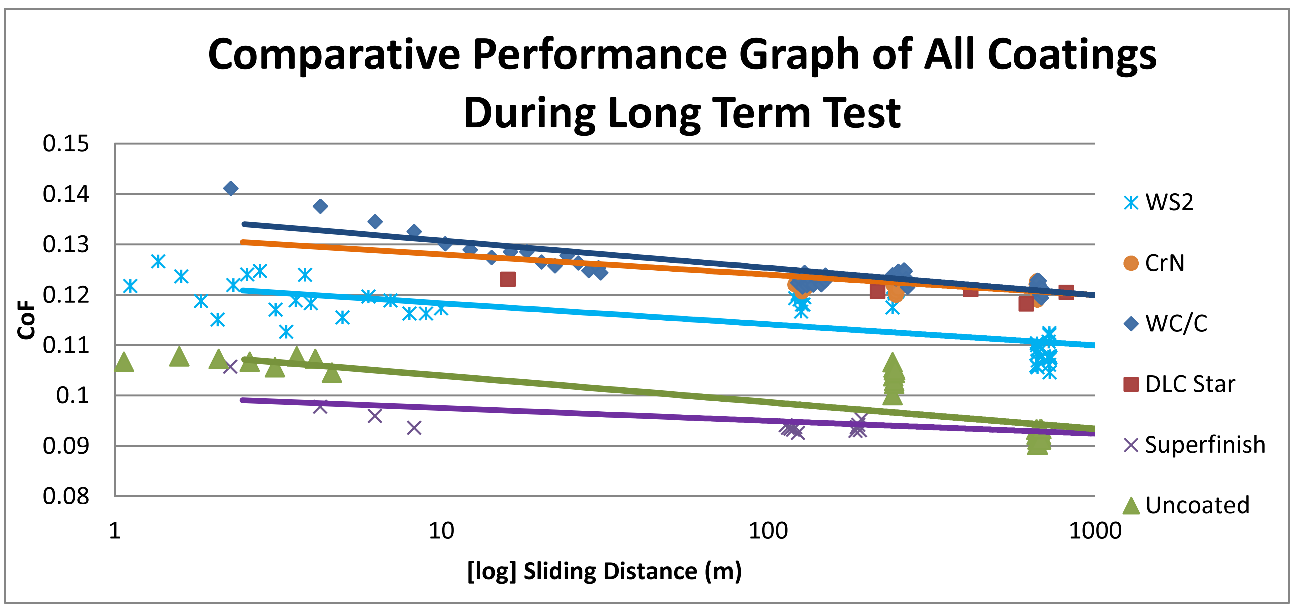

Figure 8.7 Comparative Performance Graph of all Coatings During Long Term Test

The superfinished samples are found to be the best performing candidate on a long term scale. Comparing these results to Figure 2.2 suggests that all of these samples are still within the steady state region. It is noted that the friction values of the superfinished and uncoated samples converge near the end of the test. This may indicate that the surface roughness of these samples is also converging.

As illustrated earlier in Figure 2.2, a coating failure should be noted by a change in CoF because the contacting surfaces change. If the coating was worn through, it would change to coating-substrate or substrate-substrate. While no dramatic change was noted in the CoF after the break in, which suggests no change in contact interface, the coatings on the pins had clearly worn through by the end of the test. This might indicate that the coating was worn through so quickly, that it was inseparable from break in phase of the friction plot. This would mean that the majority of the sliding was occurring on a coating-to-substrate interface.

8.3. Wear Performance

Three methods of wear measurement are common in practice – measure by weight, volume and area. Measuring by weight is very difficult because often the material loss is so small, so it requires incredibly accurate and expensive scales (measuring on the order of $1/100^{th}$ of a gram). Still there is a great deal of inaccuracy because material may deposit itself onto the substrate. Changes in weather can also affect the weight and simple repeatability is extremely difficult to control.

Measuring by volume is performed using a surface profilometer. This can be achieved with a microscope or stylus. This is feasible with equipment at the university, but requires performing extensive calculations. If the surface's original shape is known, then a subtraction of the volumes before and after can calculate the material loss. This has inherent error related to the accuracy of the original surfaces.

Lastly is the capturing of the wear scar area. This measurement was possible using the Nikon microscope available in the MSL. This too has error in the accuracy of the wear measurement as a subjective assessment needs to be made to establish the wear area. Pin samples were measured in this fashion with the Nikon AZ100 microscope and then analyzed for area measurement using NIS-Elements software, as shown in Figure 8.12.

8.3.1. Wear: Coupon

As discussed earlier in this chapter and while describing the behaviour of the tribometer, the pin reciprocates along the coupon. While the pins are being considered for the purpose of understanding which surface coating has performed the best, the coupon is valuable for gaining insight as to which velocity is of greatest concern to surface integrity. Surface imaging was performed on Zygo Newview 5000 whitelight interferometer before and after the testing. The results show that the application of the coating has slightly reduced the surface roughness of the samples before being sent out. This is likely due to the coating filling in the valleys and smoothing over some of the peaks of the original surface. The change in surface roughness depends on the thickness of the coating applied, or any pre-treatments it underwent after being sent out. The initially low surface roughness observed by the superfinished sample is a result of the processing it underwent, which was discussed in Section 5.1.5. Zygo images of these coatings are provided in the Appendix.

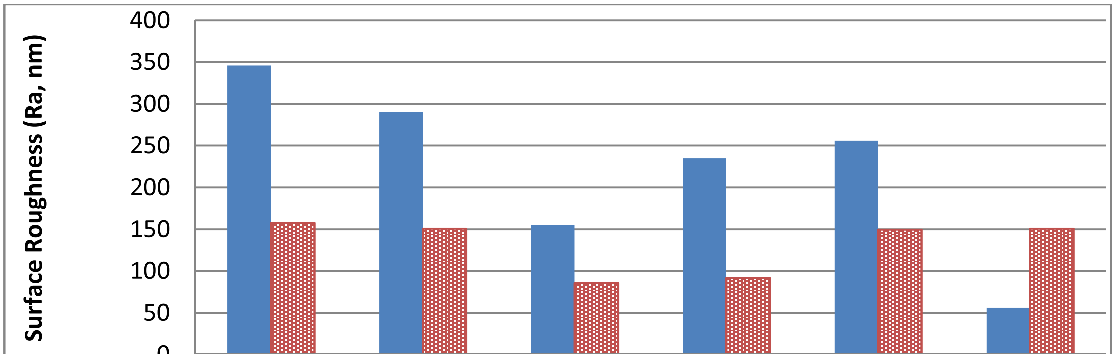

	Uncoated	CrN	WCC	WS2	DLC	Superfinish
Before	346	290	155	235	256	56
After	158	151	86	92	150	151

Figure 8.8: Coupon Surface Roughness Measurements

Figure 8.8, shown above, also shows that most of the pins experienced a polishing effect which likely occurred during the run-in stage. It can be noted that the surface roughness of the uncoated sample reduced down to 158nm and the superfinished sample increased to 151nm. This further explains the converging effect observed in the long term test.

Each position along the coupon wear track corresponds to a specific sliding velocity, with maximum values at the center and zero at the extremities. When looking at one extremity of the wear track, the center, and half-way in between to narrow down where the greatest wear exists. Surprisingly the results from these basic positions are almost indistinguishable from the other. This is so with all of the samples, as illustrated by Figures 8.9-11.

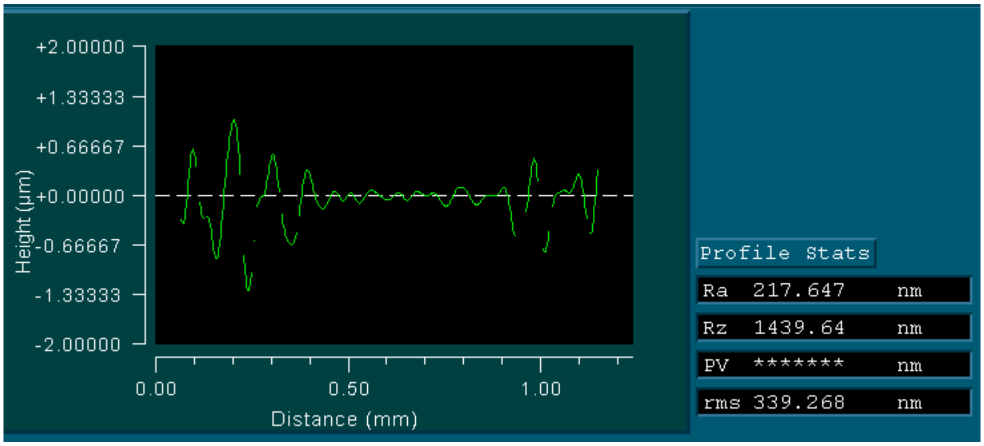

Figure 8.9 Coupon Wear -Extremity (V=0)

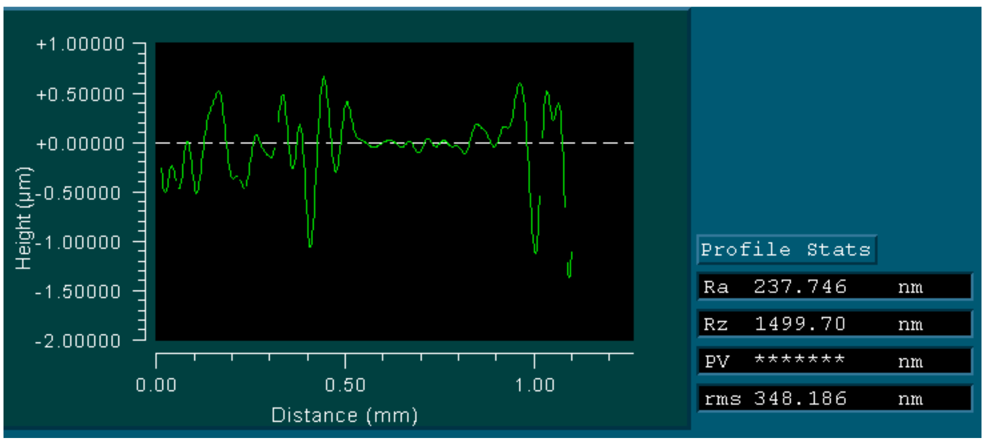

Figure 8.10Coupon Wear - Half-Way (V=50%)

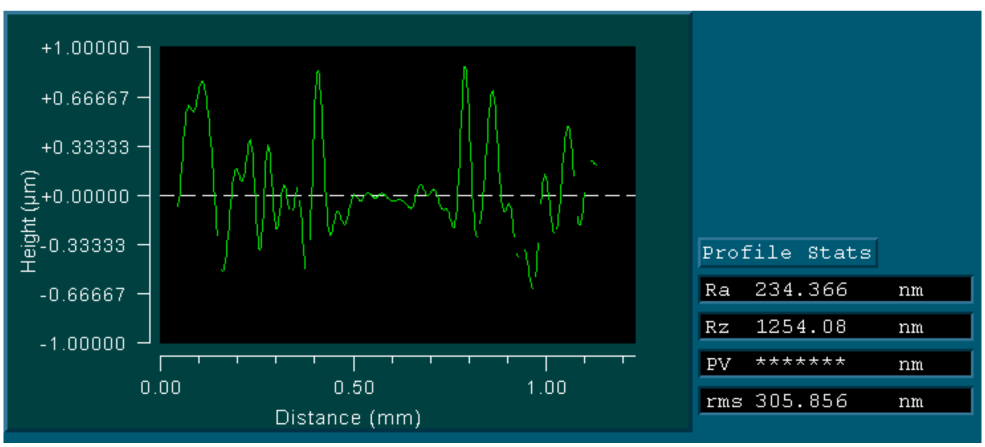

Figure 8.11 Coupon Wear -Middle (V=max)

Based on the results presented above, it would appear that the surfaces are being polished. This is determined because there seems to be no drop in height from the average along the track. Instead, the peaks and valleys have just been smoothed out. This also suggests that the lubricating fluid may not have been acting effectively in separating the sliding surfaces or that the sliding velocity was not high enough to generate a large λ.

8.3.2. Wear: Pin

Pins were selected to compare wear performance because:

1) The pins were in constant contact with the coupon. This means that it was wearing due to a long sliding distance, and experienced a range of sliding velocities. The pin may show the wear caused by a known sliding distance, while the coupon will indicate which velocity was most damaging based on the position of greatest wear along the wear track. Therefore, the pins are a focused wear scar which also sees a realistic performance spread.
2) The coupons were in intermittent contact, and observed a fraction of the wear as compared to the pins. Measuring the whole wear volume loss along the length of the coupon is not as simple or as accurate as measuring it from the pin head.

Below, in Figure 8.12, is an illustration of the wear observed on some of the pins. It is important to note that most, but not all maintain a circular and central wear scar. Occurrences such as the one below may have been caused by a misalignment of the pin with the chuck or that the coupon was not level during the test.

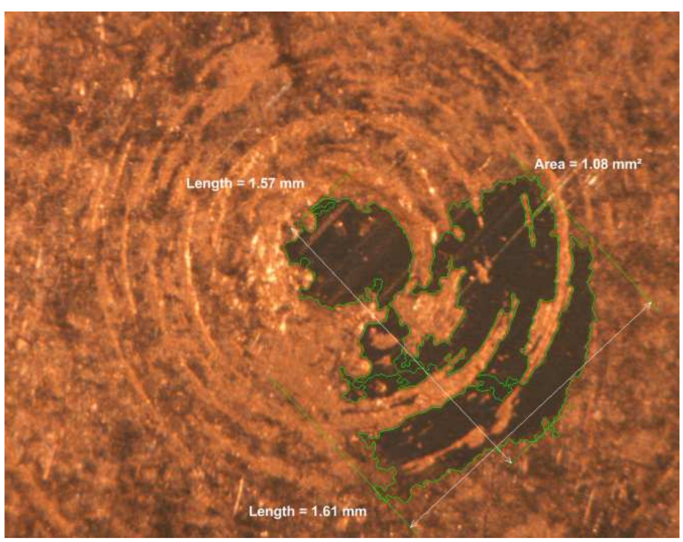

Figure 8.12 Observed Wear on Pin Head using Nikon Microscope

The overall results for the wear measured on the pins are tabulated here below in Figure 8.13:

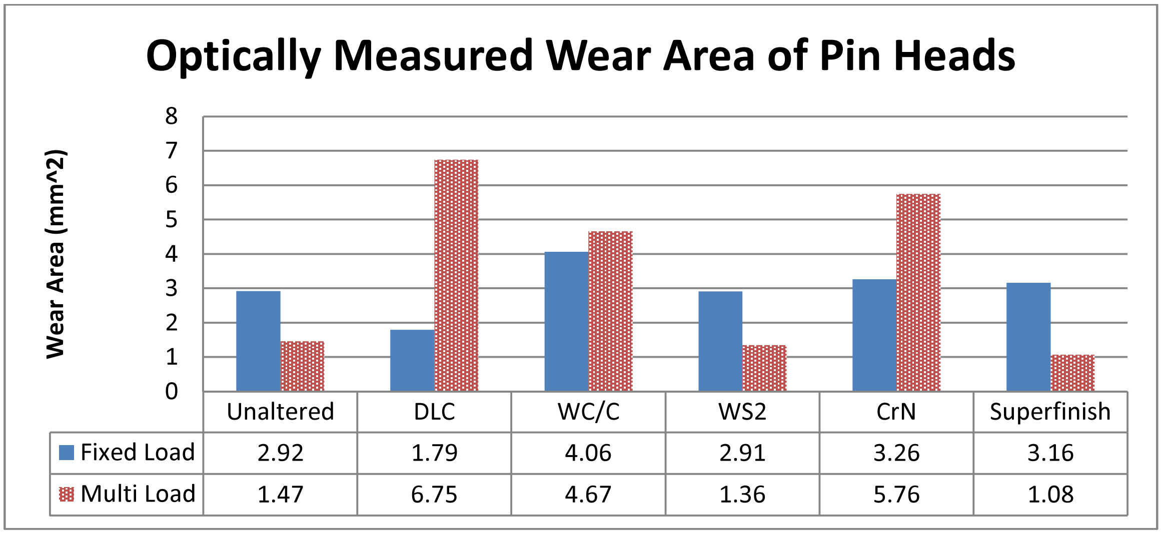

Figure 8.13 Optically Measured Wear Area of Pin Heads[3]

From Figure 8.13 shown above, the WS_2 and Superfinish samples performed the best, overall, in regards to wear resistance. Further tests on this tribometer will allow for more information to be gained about the repeatability and validity of these results.

8.4. Raman Spectroscopy

Raman Spectroscopy (RS) tests were performed to check whether chemical reactions occurred on the coating surfaces during the tribometer tests. This work was required to confirm that the coatings were in fact inert and to see if any 3rd body tribofilms were formed on the surfaces. The tests were carried out by Dr. M.D. Abad with the results discussed and related to observed performance. The RS showed that the coatings on the sample were chemically unchanged after the tests. It also confirmed that the coating applied to the pin did wear through, exposing the steel substrate, and the coupon did not.

[3] note: some of the pins did not undergo the same sliding length in the multi load tests. The uncoated and superfinished samples were not able to withstand as heavy of loads as the coated samples and were therefore not subject to the same length of sliding. This may make their wear area measurements invalid comparisons to the others.

8.5. Synchronizing Friction Data with Position

For all tests, the only data recorded is the time and the voltage output. However many of the plots are measured as a function of position or velocity. The position must be synchronized with the data in order to have meaningful data for some of the graphs. Getting an accurate synchronization of the data with respect to the position is important because it identifies which position, and which velocity, is causing the greatest friction. This is valuable for selecting a coating to work best under specific conditions.

The position function is a simple calculation operating under the rational assumption that the movement is sinusoidal. With this in place:

$$\mathrm{X_{pin}} = \mathrm{A}\sin(\omega \mathrm{t} + \emptyset) \qquad \text{Equation 8.5.1}$$

where X is the position (m), A is the amplitude (calculated by the crank arm radius. A = r_{crank} = 0.0508 m), ω is the angular velocity (RPM * 2 * pi / 60), t is the time, and ∅ is the phase angle of the function. All the variables are calculable except for the phase angle, ∅, which is left open for control to synchronize the function with the data. This phase angle will be unique for each test, but will be tuned individually by the same method for each.

Velocity is a simple derivative of the former as:

$$\frac{\mathrm{d}X_{pin}}{\mathrm{dt}} = \mathrm{V_{pin}} = \mathrm{A}\omega\cos(\omega \mathrm{t} + \emptyset) \qquad \text{Equation 8.5.2}$$

Synchronizing the data with the appropriate position will be established based on three facts.

Friction theories discussed by Richard Stribeck suggest that the maximal friction should exist where the velocity is minimal [26]. From the data, we see a near horizontal line of maximal force. Somewhere between the beginning and end of this portion should be the extremity of the position. As previously discussed in Chapter 2 and Figure 8.1 we see a small spike in the friction force as the contacts change from static to kinetic friction. This indicates that the 0 position for the pin is just slightly behind this spike. From this, an estimated bound to the position is reached. This may become more accurate as more knowledge of the physics refines the analysis.

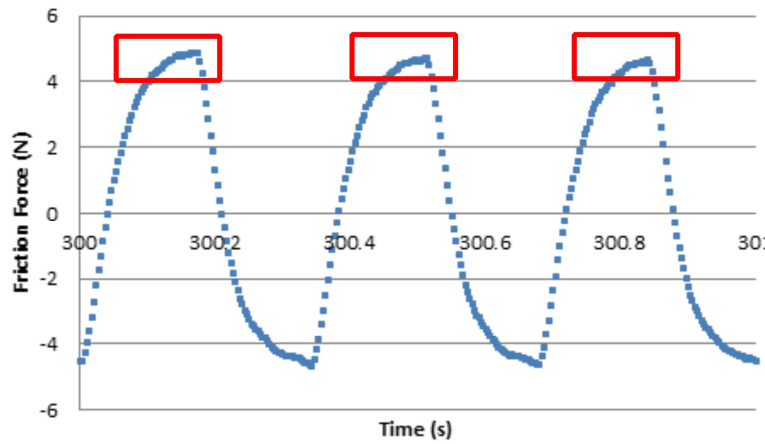

Figure 8.14 Determination of Friction Coefficient

It is also known, here in Figure 8.14, that the shape of the function should be independent of direction. When plotting a graph of Cof vs. velocity, the values should be common at each axes. Now through trial and error, an accurate synchronization of the friction values with the corresponding track position may be determined within an accuracy of ±0.1rads. This should be sufficiently accurate for the purposes of this research.

8.6. Effect of Sliding Velocity

An analysis of the influence of sliding friction on friction force was investigated. This was to bring insight into the friction mechanisms, and how they transition between eachother. This plot also helps to hone the synchronization of the friction data to the corresponding position, discussed in Section 8.5. The friction values of each cycle should start and end at the same place. Though they may not follow the same path, the behaviour of the slider is symmetric, and so should the friction.

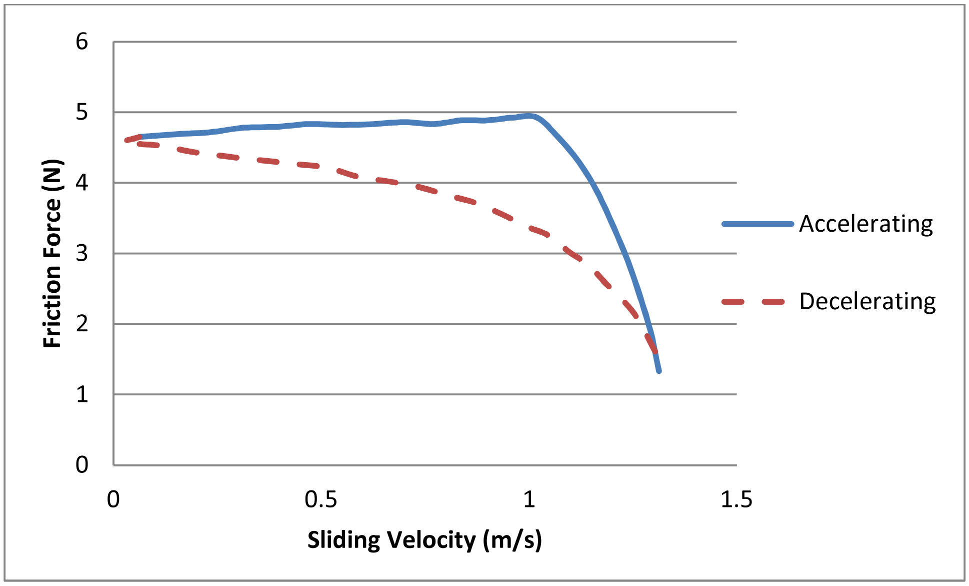

Figure 8.15 Frictional Dependence on Sliding Velocity

Figure 8.15 illustrates how the friction is reduced once a critical velocity is achieved which allows the lubricating fluid to alleviate the contact interference. Similar to the Stribeck curve, this plot also illustrates how introducing a lubricant may have significant impacts to the behaviour of friction during elevated sliding velocities.

The friction plot of the accelerating stroke has a distinct change in force after it reaches a given threshold seen at 1 m/s. The decelerating stroke does not follow this same shape because the lubricant retained between the surfaces as they slow down. The friction observed before this threshold illustrates surface sliding resistance and affirms the use of its value as the measured friction coefficient for the respective coatings.

From these tests, it is understood that friction varies heavily with sliding velocity and linearly with contact load. This also suggests that the most aggressive wear region within the motion is at the end of each stroke, when the velocity is near zero. However, it was mentioned in the tribometer sources of error that the near zero velocity positions to not necessarily simulate the pure rolling which the gears see at the pitch point.

8.7. Results Summary

The work presented here draws in all information discussed from previous chapters. Analysis of friction theory aided in the selection of surface treatments for testing. The study of gears and operating conditions were used for material selection, fabrication, as well as choosing the appropriate speeds and loads used in the multi-load and long term tests. These laboratory tests were carried in order to simulate working conditions of the transmission. The results from these tests were carried out and presented in Figure 8.3 and Figure 8.7.

Figure 8.3 and Figure 8.7 demonstrate that the uncoated and superfinished samples achieved the lowest CoF, but were not able to handle the elevated loads attempted in the multi-load test. The superfinished samples achieve a high performance because of their low surface roughness and oil entrapping features. This allows them to retain fluid within the interface and establish a more effective fluid boundary layer. Seeing as all other samples have similar roughness values, it was expected that WS_2 would be the next best performing sample. While WS_2 did show, on average, the lowest CoF of the coated samples, none of the coated samples performed significantly better than any of the others in either of the tests. A final summary of the surface treatments is collected below in Table 8.1

Table 8.1: Performance Summary of Surface Treatment Technologies

	Uncoated	Superfinish	DLC Star	Balinit C	CrN	WS2
Frictional Performance	Good	Very Good	Poor	Poor	Poor	Acceptable
Wear Resistance	Good	Good	Very Poor	Poor	Poor	Good
Cost	$0.00	$800.00	$214.08	$107.02	$56.20	$35.00
Net Env. Imp.	No change	Positive	Undetermined	Undetermined	Undetermined	Poor
Load Capacity	1.40GPa	1.40GPa	>1.50GPa	>1.50GPa	1.40GPa	>1.50GPa

The inability to withstand contact pressures above 1.5GPa may be alleviated with the incorporation of a surface coating on top of the superfinishing. Further experiments must be performed to confirm this.

Further analysis of the wear on the test pins and coupons through microscopes and Raman spectroscopy provides insight into how each of the coatings responded to tests and their ability to resist wear. Processing the data has brought insight into the role velocity has in the reduction of friction through the introduction of a lubricant, as shown in Figure 8.15.

8.8. Discussion of Results

Based on the theory studied prior, it was expected that the uncoated samples would provide the worst performance test case on every measure, and that each coating would demonstrate its tribological advantage in one area or another. Instead, the results show that none of the applied coatings had particular superiority over the uncoated, except during loads above 1.50GPa.

Measurements using the Zygo NewView 5000 whitelight interferometer indicate that the coupons only experienced a surface polishing. While the pin clearly showed coating failure, the surface of the coated coupon was not damaged. It was expected that there would be varying amounts of wear along the coupon, which may correspond to the varying sliding velocity, but the coupon showed constant wear along the sliding track. This observation suggests that pin coating failure occurred early on in the test. Once the coating failed, exposing the steel substrate, the steel continued to wear instead of the coupon.

Further study shows that some of the frictional qualities which were anticipated only exist under specific conditions. Amorphous hydrogenated carbon (a-C:H) coatings, like that found in the Balinit C coating, are capable of having a very low CoF, but specifically in vacuums or dry atmospheric conditions [62,63]. In humid or wet conditions, the CoF is distinctly higher. Similarly, many of the experiments performed with DLC coatings are mainly in dry sliding conditions. Few experiments are conducted with oil or water-based lubricants [15]. The poor performance of the coatings recorded in these tests does not disqualify the tests themselves, but brings insight into the narrow niche applications that some coatings are designed for, or that the lubricant used may be designed to work best for uncoated steel contacts. It also brings evidence to support the findings of Podgornik [15] discussed previously in Section 1.3. He reports that the lubricant itself is not able to perform as effectively as designed with the presence of a coating.

Since all of the coatings are presumed to be inert, it assumed that the lubricating fluid would not have a performance effect on one coating more than another. Even though tests show that no chemical reaction occurred on the coating surfaces, this does not imply that no chemical change occurred within lubricant. It is possible that the coating may have acted as a catalyst for chemical changes in the lubricant, or that the presence of a coating neutralized some of the additives in the lubricant; thus restricting its ability to function properly.

As shown in Figure 8.3, some coatings were actually able to perform better under higher loads. These coatings are very specialized and work best within specific operating conditions, which may be narrow or sensitive to change. This further suggests that there has to be a careful pairing of coatings with lubricants in order to achieve positive results. The Mercon V ATF was likely designed to perform best in steel-on-steel contacts.

Previous mentions, in Section 2.3, about the mechanics of wear were true with two surfaces which had large differences in hardness. Rabinowicz mentions how this becomes more complex when surfaces in contact are similar. Wear measurements were used to further compare the performance of each of the coatings. As expected, the pin wore more quickly than the coupon. The wear on the pin helped to identify which coating had the greatest wear resistance. Because the velocity was not constant, it was expected that the wear on the coupon would vary with position. Since both test pieces have the same physical properties, the coatings were worn on both the pins and coupons. This is illustrated by the surface profile results presented in Figure 8.9-12. While the coating on the pin wore through completely, the coating on the coupon also wore. This means that after the pin coating failed, there was probably an insufficient coating thickness remaining on the coupon to reduce the friction as it was intended to.

Yet, all of these reasons for poor performance bring insight into the unexpected results collected. It is peculiar to see that the coatings which were designed to reduce the friction, may be the cause for the poor results. It is important to realise from this that it is necessary to pair the correct lubricant with the correct coating, and operate within the prescribed operating conditions in order to achieve the desired improvement. These phenomena should be investigated further and resolved through more tribo-testing before being applied on the transmission.

8.9. Transmission Dynamometer

An electric motor drive train has been set up in the mechanical engineering department for research. A 30hp electric motor is connected to a Lovejoy SU-6 coupling, connected a Lebow 1228 torque sensor which is then connected to the test subject. Jeff Sylvester used this test stand, as shown in Figure 8.16, for his masters research, to model the behavior of a 4-cylinder internal combustion engine by back-driving it with the electric motor [64].

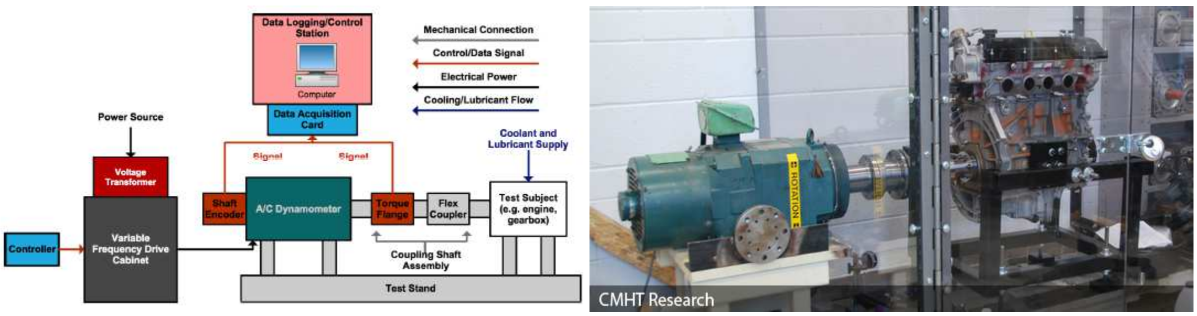

Figure 8.16 In-House Dynamometer Schematic and Setup

8.9.1. Transmission Tests / Modeling

Work completed by Professor Rao was a very important discovery for gear-box modeling [6]. The dynamometer has similar speed control as that which was expressed in Rao's research, but it has not yet been possible to control the transmission adequately; for a few reasons:

Firstly, these dynamometer tests were performed before any transmission disassembly took place. It was important to establish original performance results before any alterations took place. Because of this, there was little understanding of its exact mechanics and how it may be best controlled. Secondly, this transmission also requires the control of the electric motor in order to load all of the gears. This means that it was not possible to produce power at the output or offer back-end loads to load the gears in different ways. Testing, to date, indicates the ability of the test stand to serve as a testing apparatus for different treatments and is, thus, recommended for use in further studies of the transmissions.

With all of these problems unresolved, the drive train was not yet ready to conduct valuable tests for modeling power losses in a transmission. It has, however, operated as a successful proof of concept to encourage other research to be explored here.

In order to model the frictional dynamics of the transmission, a few important tests need to be carried out. As discussed in Section 1.2, a number of researchers document the primary contributors and methods of modelling the gear-box. Tests designed to accelerate the transmission, followed by steady state rpm offers an indication as to what component of the torsional resistance is due to the inertia of the gears inside. Back-loading the transmission as well as no-load tests help to identify the losses due to the bearings. Viscous losses can only be measured by opening the transmission, emptying the liquids and replacing the lubricant with one which has a different viscosity. The gear flank face friction can be calculated using the data from the loaded tests, and removing the contributions from all other losses. This can be expressed mathematically by balancing the torque in by the torque out:

$$T_{in} = T_{inertia} + T_{bearing} + T_{fluid} + T_{flank} + T_{out} \qquad \text{Equation 8.9.1}$$

with the T_{out} measured by a load cell, and all the other torque losses modelled, T_{flank} is the remaining term to be solved. With this data, the contact loads for each gear tooth can be calculated, and then the coefficient of friction on the flank face can be estimated.

8.9.2. Outcome

Simple multi-speed tests were run with the transmission, as a proof-of-concept and to explore the capabilities of the system. As the system had never been used before, these were conducted simply for a proof-of-concept; so do not have technical validity to the research. For this reason there was not extensive analysis done on the data output other than to demonstrate and understand the workings of the system.

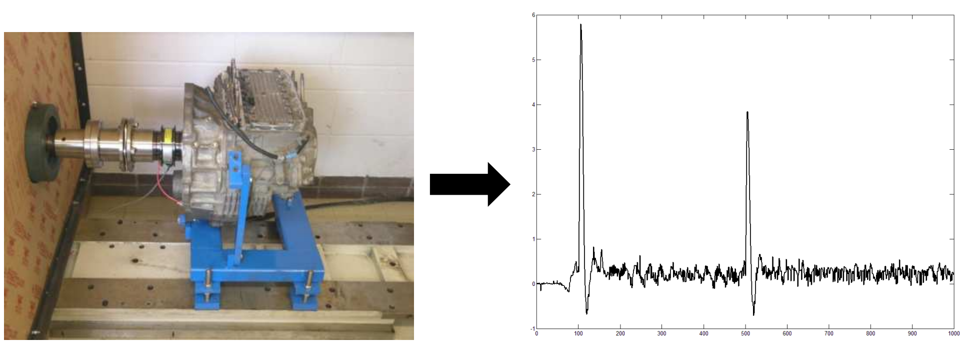

Figure 8.17 Torsional Resistance Measured During Multi-Speed Test on the Dynamometer

Data collected, like Figure 8.17 Torsional Resistance Measured During Multi-Speed Test on the Dynamometer, show the torsional resistance the torque sensor a multi-speed tests. Initially at rest for one second, the transmission input shaft was accelerated to 100RPM, held at this speed for five seconds, then accelerated up to 150RPM, and held at this speed also for 10 seconds. This short test demonstrates the simple control and data acquisition available on the system. This simple test illustrates how the torsional resistance observed can be used to calculate specific internal parameters of the transmission. For example, these sudden spikes are due to the acceleration of the gears inside and the torque required for acceleration and can be used to calculate their moment of inertia. It also illustrates the insignificant change in torsional resistance between one constant speed and another. This further supports that acceleration sees significantly higher loads than a steady-state circumstance. Given more time for study, this apparatus would have been used for full scale modelling of the transmission.

While the results from this test were not included for analysis, the test itself demonstrates a working test platform which allows for speed control and data acquisition of torsional resistance. This proof-of-concept encourages the in-house dynamometer to be used for future research projects.

Conclusion

In summary, this research has taken a step forward to test surface coatings which may be used to improve vehicle performance and reduce the environmental impact of the automotive industry.

A mathematical model has been successfully used to calculate the bounds and behavior of the sliding velocity and contact pressure for helical gear teeth. An approach to evaluating additional factors, such as cost and environmental considerations, has been mentioned which brings additional factors into the coating selection process. From which, five surface treatment applications were selected to observe their tribological performance and how they compare to unaltered (uncoated) and current industrial (WS_2) benchmarks.

The calculated loads and speeds were used as the conditions for which coated pins and coupons were tested. Multi-Load and Long-Term tests have been performed and their results have been presented above, which show shot-peening/super-finishing has the best frictional performance under 1.40 GPa. This is due to its retention of the lubricant within the low velocity region.

Further tests can be performed in future to expand the selection of coatings, and vary the operating conditions to observe the coating performance. C.A.S.E processing is illustrated as being a valuable and environmentally friendly option to minimize the friction observed between gear teeth.

A dynamometer has been successfully built for use to model the full-system modeling of the hybrid transmission. This is the final stage in the research process to confirm that the tribological improvements observed in the controlled environment are transferrable to full-system operation.

Future Work

A dynamometer has been installed at McMaster, and should be used for full system testing of the original transmission (unaltered). Tests should be run to isolate the loss components, as outlined in Section 1.2. Multi-load and multi-speed tests can be done to model the bearing and gear losses. All of this work is only possible once the transmission can be loaded and electronically controlled for the electric motors. Since the study focusses on any gear tooth interaction, it would be simpler to test and model gears in a manual transmission.

Future work can be directed at the exploration of other coatings and combinations of surface technologies. This can be done with the prospective coatings on top of the CASE polished samples. The operating conditions have been set and the important factors for coating selection have been established. It is important to emphasize the use of the coating on only one of the interfaces. And to use a tribometer which offers more reliable and repeatable data. A tribometer which effectively simulates the low velocity sliding and rolling under heavy loads would be most beneficial to the study. Once a surface treatment has been chosen, it should then be tested on the transmission to model and compare the performance to its original state. Once a coating has been proven to be effective in reducing friction, it must be evaluated for its environmental hazards in order to satisfy the final criteria. It must be shown to offer positive environmental benefit and financial benefit to both the producer and consumer. Chapter 4 and Regulation 347 outline the necessary procedures to carry forward. However, it is suggested that efforts would be better used exploring lubricating fluids and testing environmentally friendly base oils; as this may have a greater impact on friction reduction.

Appendix

SEM test result:

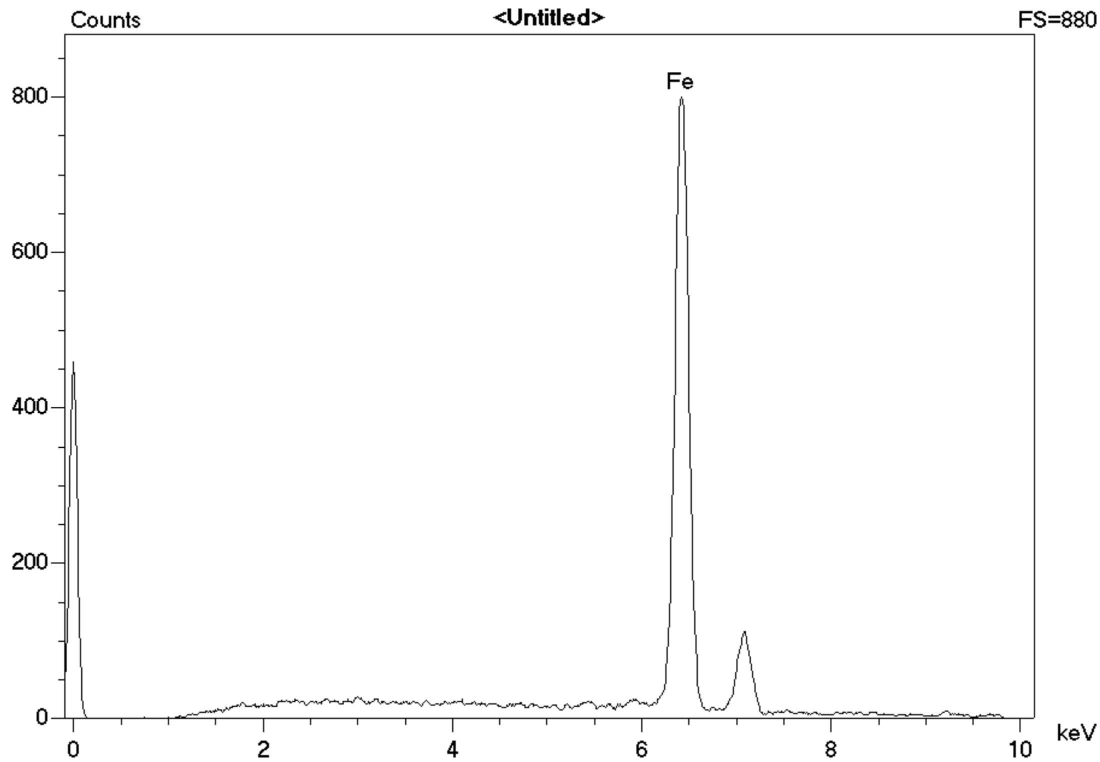

GDOES Results:

Gear 3

Element	Result	RSD	Measur.1	Measur.2	Measur.3
Fe - 372	97.205	0.003	97.203	97.205	97.208
C - 156	0.212	0.720	0.210	0.212	0.213
Mn - 403	0.877	0.500	0.882	0.875	0.873
Mo - 386	0.192	0.220	0.192	0.191	0.191
Ti - 365	0.001	13.000	0.001	0.001	0.001
Cr - 425	0.424	0.510	0.426	0.424	0.422
Ni - 341	0.573	0.400	0.571	0.573	0.576
Cu - 325	0.096	0.450	0.096	0.096	0.096
P - 178	0.023	0.680	0.023	0.023	0.023
S - 181	0.016	0.760	0.016	0.016	0.016
Nb - 316	0.095	0.250	0.095	0.095	0.095
Si - 288	0.230	0.074	0.230	0.230	0.229
Sn - 318	0.000	140.000	0.000	0.000	0.000
B - 250	0.000	140.000	0.000	0.000	0.000
Al - 396	0.040	0.720	0.040	0.040	0.040
V - 438	0.006	3.000	0.006	0.006	0.006

Gear 8

Element	Result	RSD	Measur.1	Measur.2	Measur.3
Fe - 372	97.037	0.010	97.030	97.032	97.048
C - 156	0.221	0.550	0.220	0.220	0.222
Mn - 403	0.809	0.430	0.812	0.810	0.805
Mo - 386	0.189	0.540	0.190	0.188	0.188
Ti - 365	0.001	10.000	0.001	0.002	0.002
Cr - 425	1.063	0.340	1.066	1.063	1.059
Ni - 341	0.075	0.230	0.075	0.075	0.075
Cu - 325	0.158	0.310	0.158	0.158	0.159
P - 178	0.031	1.300	0.031	0.032	0.031
S - 181	0.020	4.000	0.019	0.020	0.021
Nb - 316	0.100	0.380	0.100	0.100	0.099
Si - 288	0.226	0.380	0.224	0.228	0.225
Sn - 318	0.000	170.000	0.000	0.000	0.000
B - 250	0.000	19.000	0.000	0.000	0.000
Al - 396	0.042	0.540	0.042	0.042	0.041
V - 438	0.010	3.900	0.010	0.010	0.010

Element	Result	RSD	Measur.1	Measur.2	Measur.3
Fe - 372	97.210	0.005	97.205	97.211	97.214
C - 156	0.208	0.440	0.208	0.209	0.209
Mn - 403	0.870	0.300	0.872	0.869	0.867
Mo - 386	0.192	0.210	0.192	0.192	0.191
Ti - 365	0.001	7.300	0.001	0.001	0.001
Cr - 425	0.422	0.550	0.424	0.422	0.420
Ni - 341	0.578	0.140	0.579	0.578	0.577
Cu - 325	0.096	0.150	0.096	0.096	0.096
P - 178	0.024	0.700	0.024	0.024	0.024
S - 181	0.016	11.000	0.014	0.016	0.018
Nb - 316	0.095	0.220	0.095	0.095	0.095
Si - 288	0.231	0.310	0.232	0.231	0.231
Sn - 318	0.000	0.800	0.000	0.000	0.000
B - 250	0.000	0.800	0.000	0.000	0.000
Al - 396	0.040	1.000	0.040	0.040	0.039
V - 438	0.005	5.500	0.006	0.005	0.005

Element	Result	RSD	Measur.1	Measur.2	Measur.3
Fe - 372	97.031	0.013	97.022	97.026	97.046
C - 156	0.225	0.470	0.224	0.225	0.226
Mn - 403	0.804	0.480	0.807	0.804	0.800
Mo - 386	0.191	0.670	0.192	0.191	0.189
Ti - 365	0.002	11.000	0.002	0.002	0.002
Cr - 425	1.070	0.630	1.075	1.072	1.062
Ni - 341	0.075	0.390	0.075	0.075	0.075
Cu - 325	0.161	1.100	0.161	0.163	0.159
P - 178	0.033	0.190	0.033	0.033	0.033
S - 181	0.021	1.400	0.021	0.020	0.021
Nb - 316	0.099	0.140	0.099	0.099	0.099
Si - 288	0.226	0.320	0.226	0.226	0.225
Sn - 318	0.000	170.000	0.000	0.000	0.000
B - 250	0.000	10.000	0.000	0.000	0.000
Al - 396	0.042	0.680	0.042	0.041	0.042
V - 438	0.010	1.300	0.010	0.010	0.010

Coupon Surface Roughness Measurements Using Zygo

WS_2	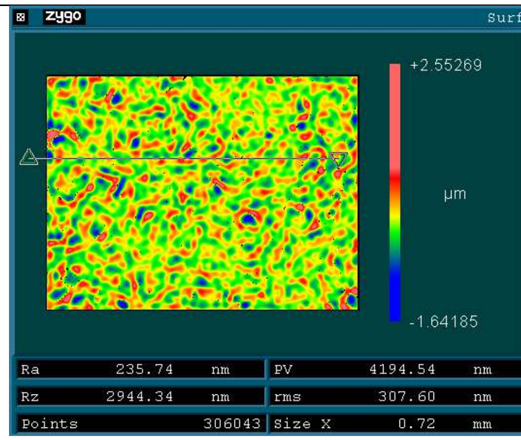
CrN	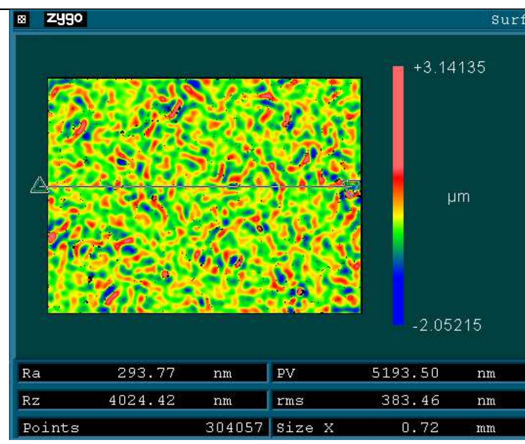

<table>
<tr><td>WC/C</td><td></td><td>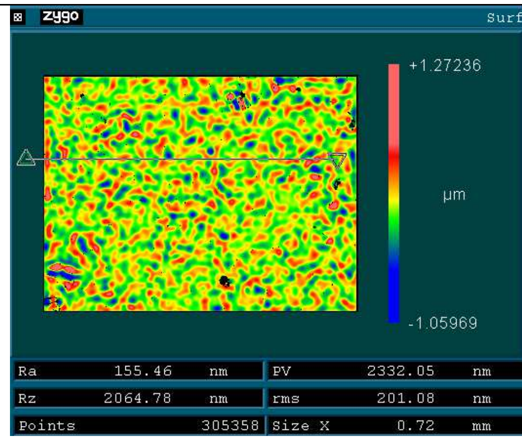
</td></tr>
<tr><td>DLC</td><td></td><td>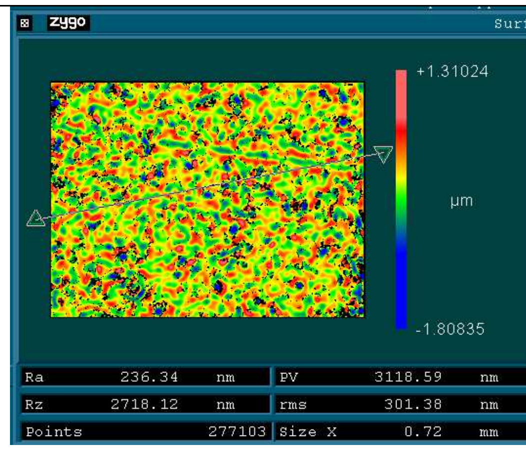
</td></tr>
<tr><td>Superfinish</td><td></td><td>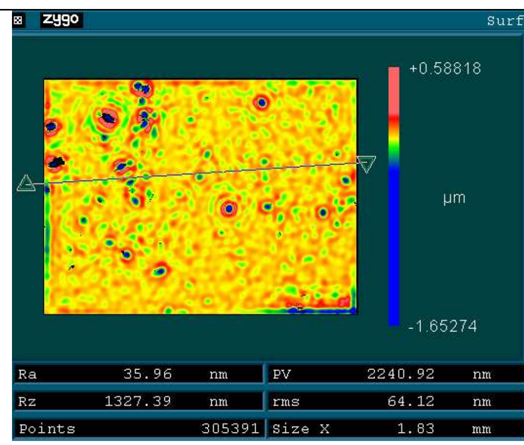
</td></tr>
</table>

Uncoated		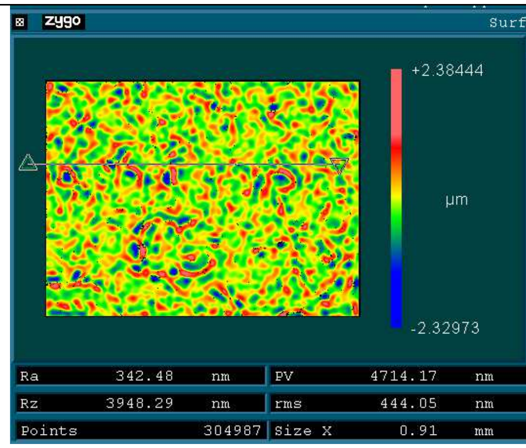zygo
Surfa
+2.38444
µm
-2.32973
Ra 342.48 nm
PV 4714.17 nm
Rz 3948.29 nm
rms 444.05 nm
Points 304987
Size X 0.91 mm

Bibliography

[1] G. Fenske, R. Erck, L. Ajayi, A. Erdemir, O.Eryilmaz ‘Parasitic Energy Loss Mechanisms Impact on Vehicle System Efficiency, Project 15171Argonne National Laboratory, April 18-20-2006.

[2] Sell, David J. "Finite Element Modeling Spur and Helical Gears in Contact." International Truck and Bus Meeting and Exposition, November 16, 1992 - November 19. 1992.

[3] Hassan, Ali Raad. "Contact Stress Analysis of Spur Gear Teeth Pair." World Academy of Science, Engineering and Technology 58 (2009): 611-6.

[4] Buckingham, Earle. Analytical Mechanics of Gears. McGraw-Hill Book Co., 1949.

[5] Merrit. Gears. Issac Pitman Publication, 1966.

[6] Rao, A. C. "Friction Coefficients for Involute Gear Drives." Journal of the Institution of Engineers (India): Mechanical Engineering Division 56 (1975): 67-70.

[7] Mihalidis, A., et al. "Prediction of the Friction Coefficient of Spur Gear Pairs."

[8] Martins, R., R. Amaro, and J. Seabra. "Influence of Low Friction Coatings on the Scuffing Load Capacity and Efficiency of Gears." Tribology International 41.4 (2008): 234-43.

[9] Weck M, Hurasky-Schonwerth O, Bugiel C. Service behaviour of PVD-coated gearing lubricated with biodegradable synthetic ester oils. VDI-Ber 2002;1665.

[10] F. Joachim, N. Kurz, B. Glatthaar Influence of coatings and surface improvements on the lifetime of gears VDI Ber, 2 (1665) (2002), pp. 565–582

[11] Höhn B-R, Michaelis K, Vollmer T. Thermal rating of gear drives: balance between power loss and heat dissipation. AGMA technical paper, 1996.

[12] R. Amaro *et al.* Molybdenium disulfide/titanium low friction coating for gears application Tribol Int, 38–4 (2004), pp. 423–43.

[13] R. Amaro *et al.* Carbon/chromium low friction surface coating for gears application Ind Lubr Tribol, 57 (6) (2005).

[14] Amaro R, et al. MoST low friction coating for gears application. In: Proceedings of GEARS 2003—gears and transmissions workshop, 2003, FEUP-Porto-Portugal.

[15] Podgornik, B., et al. "Tribological Behaviour of WC/C Coatings Operating Under Different Lubrication Regimes." 30th International Conference on Metallurgical Coatings and Thin Films.

[16] Wahl, K.J. "Role of the Third Body in Life Enhancement of MoS_2." Elsevier Science B.V. (1996): 407-413.

[17] Xiao, Li. Gear Tribology - Friction and Surface Topography. PhD Thesis. Göteborg, Sweden: Chalmers University of Technology, 2005.

[18] Alanou, M. P., H. P. Evans and R. W. Snidle. "Effect of Different Surface Treatments and Coatings on the Scuffing Performance of Hardened Steel Discs at very High Sliding Speeds." .

[19] Kozma, M. "Investigation into the Scuffing Load Capacity of Environmentally-Friendly Lubricating Oils." Journal of Synthetic Lubrication 14.3 (1997): 249-58.

[20] Kalin, Mitjan, et al. "The Lubrication of DLC Coatings with Mineral and Biodegradable Oils having Different Polar and Saturation Characteristics." Surface and Coatings Technology 200.14-15 (2006): 4515-22.

[21] STLE Conference Presentation "Environmentally Safe Lubricants; Features, Benefits and Uses" M.E. Miller May 7, 2012

[22] Shaw, Milton C. "Metal Cutting Principles." New York: Oxford University Press, 2004.

[23] Rabinowicz, Ernest. Friction and Wear of Materials, Second Edition. New York: John Wiley & Sons Inc., 1995.

[24] Stachowiak, Gwidon W. Wear: Materials, Mechanisms and Practice. John Wiley & Sons, Ltd., 2005

[25] Booser, Richard E. and American Society of Lubrication Engineers. Handbook of Lubrication: Theory and Practice of Tribology. Volume 2. Theory and Design. CRC Press, 1983.

[26] Bowden, Frank Philip., Tabor, David. Friction and Lubrication. London: Barnes & Noble, 1967.

[27] Maitra, Gitin M. Handbook of Gear Design. 2. Tata McGraw-Hill, 1994.

[28] Brain, Marshall. "How Manual Transmissions Work" 1 April 2000. HowStuffWorks.com. <http://auto.howstuffworks.com/transmission.htm> 1 May 2012.

[29] Shigley, Joseph E. and Charles R. Mischke. Mechanical Engineering. New York: McGraw-Hill, 1988.

[30] Ford Motor Company. n.d. 20 February 2011 <http://www.ford.com/suvs/escape/specifications/engine/>.

[31] Davis, Joseph R. Gear Materials, Properties, and Manufacture. ASM International, 2005.

[32] Budynas, Richard G. Shigley's Mechanical Engineering Design, 8th Ed. New York: McGraw-Hill, 2008.

[33] Norton, R.L. Machine DesignL An Integrated Approach, 3rd Ed. Prentice Hall, 2006.

[34] Flasker, Joze, Srecko Glodez, and Stanislav Pehan. "Influence of Functional Contact Area on the Stress Field in a Gear Tooth Root; Journal of Mechanical Engineering 39.11-12 (1993): 299-308.

[35] Litvin, F.L., et al. "Application of Finite Element Analysis for Determination of Load Share, Real Contact Ratio, Precision of Motion, and Stress Analysis." Journal of Mechanical Design (1996): 561-567.

[36] Song He, Sungmin Cho and Rajendra Singh. "Prediction of Dynamic Friction Forces in Spur Gears Using Alternate Sliding Friction Formulations." Journal of Sound and Vibration 309.3-5 (2008): 843-851.

[37] Ford Motor Company. "MSDS: Mervon V Automatic Transmission Fluid." MSDS Official Record. 2004.

[38] DuBois, Dr. David D. and Dr. Edmund Rodrigues. Discussion of Waste Classification: Regulation 347 DuBois. 8 January 2010.

[39] Brycoat. Brycoat Inc. . n.d. 25 October 2010 <http://www.brycoat.com/coating-services/dry-film-lubricant-coating/ws2.html>.

[40] Brycoat. Brycoat Inc. . n.d. 25 October 2010 <http://www.brycoat.com/coating-services/pvd-coatings/chromium-nitride-crn.html>.

[41] Amaro, R.I. "Carbon/Chromium low friction surface coating for gears application" *Industrial Lubrication and Technology.* v 57, n 6, p 233-242, 2005

[42] Xiao, Li "Gear Tribology- Friction and Surface Topography" Department of Materials and Manufacturing Technology, Chalmers University of Technology, Götenborg, Sweden, 2005.

[43] Zhang, Jinyu, and Yonggang Meng. "Direct Observation of Cavitation Phenomenon and Hydrodynamic Lubrication Analysis of Textured Surfaces." Tribology Letters 46.2 (2012): 147-58.

[44] Wang, Xiaolei, et al. "Optimization of the Surface Texture for Silicon Carbide Sliding in Water." Applied Surface Science 253.3 (2006): 1282-6.

[45] Etsion, I. "Improving Tribological Performance of Mechanical Components by Laser Surface Texturing." Smart Surfaces in Tribology: Advanced Additives and Structured Surfaces Conference. 10-12 Sept. 2003.

[46] Ryk, G., Y. Kligerman, and I. Etsion. "Experimental Investigation of Laser Surface Texturing for Reciprocating Automotive Components." Tribology Transactions 45.4 (2002): 444-9.

[47] Wakuda, M., et al. "Effect of Surface Texturing on Friction Reduction between Ceramic and Steel Materials Under Lubricated Sliding Contact." Wear 254.3-4 (2003): 356-63.

[48] Tovey, J. (2010). *Electrical Discharge Texturing of Cutting Tools*.

[49] Hassan, Ali Raad “Contact Stress Analysis of Spur Gear Teeth Pair” World Academy of Science, Engineering and Technology, 2009

[50] Metal Improvements Company. "Shot Peening Applications." Technical Manual. 2005.

[51] Metal Improvements Company. "C.A.S.E Isotropic Finishing Process." 2006.

[52] STLE Conference Presentation “Micromechanical and Tribological Characterization of Polymeric-based Coatings” Seung Min Yeo, May 10, 2012

[53] Momentive. Boron Nitride (hBN) Powder. n.d. 15 October 2010 <http://www.momentive.com/Products/Main.aspx?id=22818>.

[54] Dupont. Teflon Coatings: Six Basic Types. n.d. 15 October 2010 <http://www2.dupont.com/Teflon_Industrial/en_US/products/selection_guides/coatings.html >.

[55] Dupont. Flouropolymer Comparison – Typical Properties. n.d. 15 October 2010 <http://www2.dupont.com/Teflon_Industrial/en_US/tech_info/techinfo_compare.html?src=teflon-ptfe-properties >.

[56] Orion. Orion FlouroMed Coating List. n.d. 15 October 2010 <http://www.orioncoat.com/fluoromed-coating-list >.

[57] Lower Friction. Lower Friction. n.d. 16 October 2010 <http://www.lowerfriction.com/product-page.php?categoryID=1>.

[58] Lower Friction. "MSDS: Tungsten Disulfide WS2." MSDS Official Record. 2008.

[59] ASTM Standard D5182, 2002 (2008), "Standard Test Method for Evaluating the Scuffing Load Capacity of Oils (FZG Visual Method)," ASTM International, West Conshohocken, PA

[60]Falex. "Pin & Vee Block Testing Machine." Operators Manual. 2010. <http://www.falex.com/pdf/FalexPinVeeBlock.pdf>.

[61] Omega. Low Profile Bending Beam Load Cells. n.d. 10 May 2012 <http://www.omega.com/pptst/LCDA.html>.

[62] A. Erdemir, M. Halter, G.R. Fenske, et. al. Trib. Transaction 40 (1997) 667-675.

[63] A. Erdimir, Surf. Coat. Technol. 146-147 (2001) 292-297.

[64] Sylvester, Jeffrey. Characterization and Modeling of Rubbing Friction a Motored Four-Cylinder Internal Combustion Engine. M.A.Sc. Thesis. Hamilton: McMaster University, 2011.